Case Study: Comparison Between LHC and ESRF Synchrotron Radiation Power, Fluxes and Spectra and Related Effects on Their Vacuum Systems

R. Kersevan, TE/VSC-VSM – CERN, Geneva

Agenda:

- This tutorial on synchrotron radiation (SR) will use two existing accelerators, of different purpose, **as examples of SR sources of completely different nature**;

- The aim is to show how these differences affect the design and operation of their respective vacuum systems;

- A short introduction to the formalism of SR theory and some relevant formulae is given;

- The two accelerators are: **LHC** p-p collider at CERN, Geneva, and the **ESRF** synchrotron radiation light source, located in Grenoble, France;

- It will be shown how the fact that one has protons as the source and one electrons greatly influences the properties of the SR they generate, and the way their vacuum systems are designed;

- Relevant formulae are then applied to the two machines, and peculiar features are discussed;

- Conclusions;

- References to documents easily found on internet are given during the tutorial.

Sources: Schwinger; Sokolov-Ternov;

PHYSICAL REVIEW — VOLUME 75, NUMBER 12 — JUNE 15, 1949

On the Classical Radiation of Accelerated Electrons

JULIAN SCHWINGER
Harvard University, Cambridge, Massachusetts
(Received March 8, 1949)

This paper is concerned with the properties of the radiation from a high energy accelerated electron, as recently observed in the General Electric synchrotron. An elementary derivation of the total rate of radiation is first presented, based on Larmor's formula for a slowly moving electron, and arguments of relativistic invariance. We then construct an expression for the instantaneous power radiated by an electron moving along an arbitrary, prescribed path. By casting this result into various forms, one obtains the angular distribution, the spectral distribution, or the combined angular and spectral distributions of the radiation. The method is based on an examination of the rate at which the electron irreversibly transfers energy to the electromagnetic field, as determined by half the difference of retarded and advanced electric field intensities. Formulas are obtained for an arbitrary charge-current distribution and then specialized to a point charge. The total radiated power and its angular distribution are obtained for an arbitrary trajectory. It is found that the direc-

tion of motion is a strongly preferred direction of emission at high energies. The spectral distribution of the radiation depends upon the detailed motion over a time interval large compared with the period of the radiation. However, the narrow cone of radiation generated by an energetic electron indicates that only a small part of the trajectory is effective in producing radiation observed in a given direction, which also implies that very high frequencies are emitted. Accordingly, we evaluate the spectral and angular distributions of the high frequency radiation by an energetic electron, in their dependence upon the parameters characterizing the instantaneous orbit. The average spectral distribution, as observed in the synchrotron measurements, is obtained by averaging the electron energy over an acceleration cycle. The entire spectrum emitted by an electron moving with constant speed in a circular path is also discussed. Finally, it is observed that quantum effects will modify the classical results here obtained only at extraordinarily large energies.

EARLY in 1945, much attention was focused on the design of accelerators for the production of very high energy electrons and other charged particles.[1] In connection with this activity, the author investigated in some detail the limitations to the attainment of high energy electrons imposed by the radiative energy loss[2] of the accelerated electrons. Although the results of this work were communicated to various interested persons,[1,3,4] no serious attempt at publication[5] was made. However, recent experiments on the radiation from the General Electric synchrotron[6] have made it desirable to publish the portion of the investigation that is concerned with the properties of the radiation from individual electrons, apart from the considerations on the practical attainment of very high energies. Accordingly, we derive various properties of the radiation from a high energy accelerated electron; the comparison with experiment has been given in the paper by Elder, Langmuir, and Pollock.

I. GENERAL FORMULAS

Before launching into the general discussion, it is well to notice an elementary derivation of the total rate of radiation, based on Larmor's classical formula for a slowly moving electron, and arguments of relativistic invariance. The Larmor formula for the power radiated by an electron that

is instantaneously at rest is

$$P = \frac{2}{3}\frac{e^2}{c^3}\left(\frac{d\mathbf{v}}{dt}\right)^2 = \frac{2}{3}\frac{e^2}{m^2c^3}\left(\frac{d\mathbf{p}}{dt}\right)^2. \quad (\text{I.1})$$

Now, radiated energy and elapsed time transform in the same manner under Lorentz transformations, whence the radiated power must be an invariant. We shall have succeeded in deriving a formula for the power radiated by an electron of arbitrary velocity if we can exhibit an invariant that reduces to (I.1) in the rest system of the electron. To accomplish this, we first replace the time derivative by the derivative with respect to the invariant proper time. The differential of proper time is defined by

$$ds^2 = dt^2 - 1/c^2(dx^2 + dy^2 + dz^2),$$

or

$$ds = (1 - v^2/c^2)^{\frac{1}{2}}dt. \quad (\text{I.2})$$

Secondly, we replace the square of the proper time derivative of the momentum by the invariant combination

$$(d\mathbf{p}/ds)^2 - 1/c^2(dE/ds)^2.$$

Hence, as the desired invariant generalization of (I.1), we have

$$P = \frac{2}{3}\frac{e^2}{m^2c^3}\left[\left(\frac{d\mathbf{p}}{ds}\right)^2 - \frac{1}{c^2}\left(\frac{dE}{ds}\right)^2\right]$$

$$= \frac{2}{3}\frac{e^2}{m^2c^3}\left(\frac{E}{mc^2}\right)^2\left[\left(\frac{d\mathbf{p}}{dt}\right)^2 - \frac{1}{c^2}\left(\frac{dE}{dt}\right)^2\right]. \quad (\text{I.3})$$

The conventional form of this result is obtained on

[1] See L. I. Schiff, Rev. Sci. Inst. 17, 6 (1946).
[2] D. Iwanenko and I. Pomeranchuk, Phys. Rev. 65, 343 (1944).
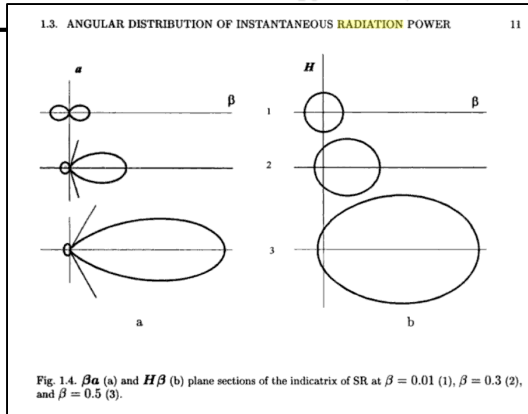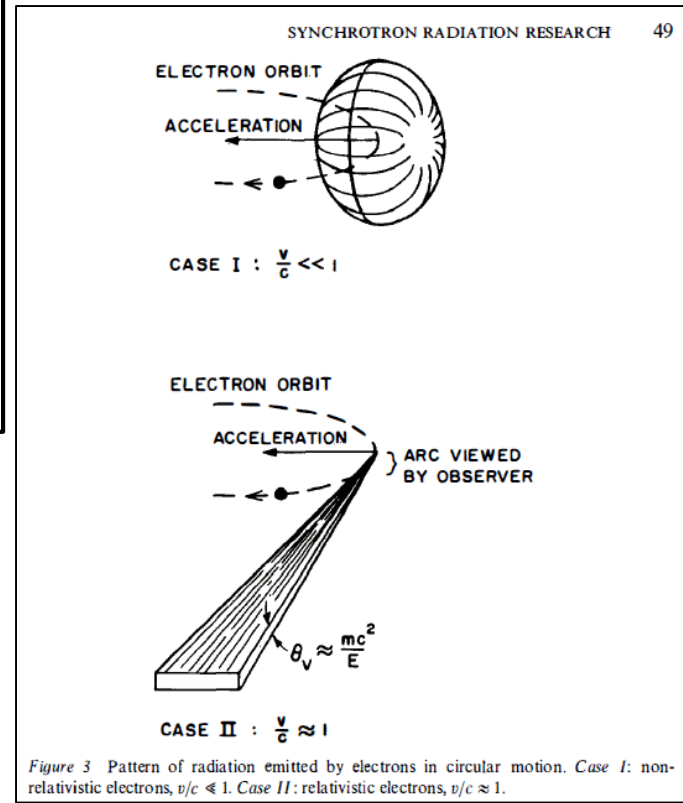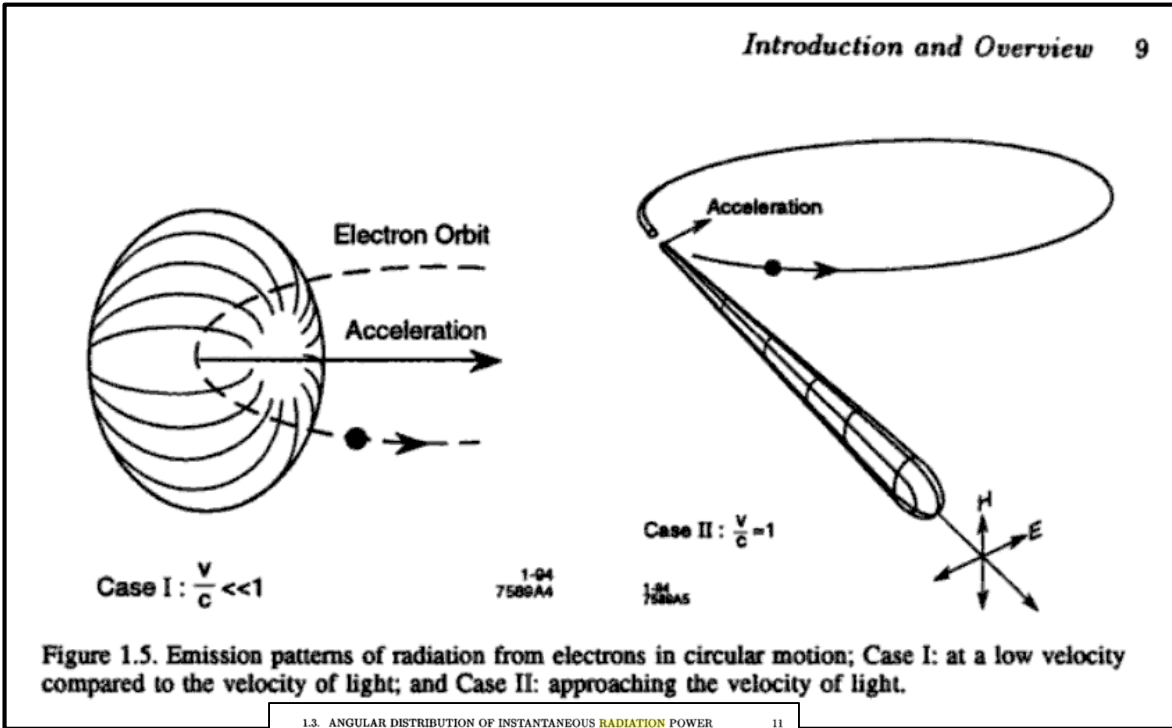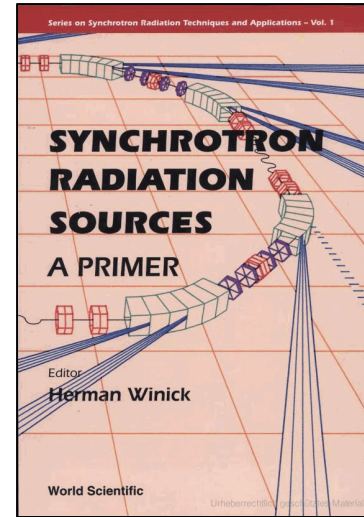[3] Edwin M. McMillan, Phys. Rev. 68, 144 (1945).
[4] John P. Blewett, Phys. Rev. 69, 87 (1946).
[5] Julian Schwinger, Phys. Rev. 70, 798 (1946).
[6] Elder, Langmuir, and Pollock, Phys. Rev. 74, 52 (1948).

1912

Fundamental paper by J Schwinger: it gave for the first time quantitative and qualitative insights into the properties of radiation emitted by relativistic charged particles moving in a magnetic field.

Followed by second paper…

PHYSICAL REVIEW D — VOLUME 7, NUMBER 6 — 15 MARCH 1973

Classical Radiation of Accelerated Electrons. II. A Quantum Viewpoint*

Julian Schwinger
University of California, Los Angeles, California 90024
(Received 27 November 1972)

The known classical radiation spectrum of a high-energy charged particle in a homogeneous magnetic field is rederived. The method applies, and illuminates, an exact (to order α) expression for the inverse propagation function of a spinless particle in a homogeneous field. An erratum list for paper I is appended.

… while in the meantime <u>Sokolov and Ternov</u> in the USSR had come to similar results expanding the breadth of knowledge (radiative polarization of electrons and positrons in a magnetic field).

As the velocity v increases, <u>the emission of photons</u> from an electron subjected to an acceleration perpendicular to its velocity vector changes and goes from being "isotropic" to being highly skewed and collimated in the forward direction

Introduction and Overview 9

Figure 1.5. Emission patterns of radiation from electrons in circular motion; Case I: at a low velocity compared to the velocity of light; and Case II: approaching the velocity of light.

Case I : $\frac{v}{c} \ll 1$

Case II : $\frac{v}{c} \approx 1$

1.3. ANGULAR DISTRIBUTION OF INSTANTANEOUS RADIATION POWER 11

Fig. 1.4. βa (a) and $H\beta$ (b) plane sections of the indicatrix of SR at $\beta = 0.01$ (1), $\beta = 0.3$ (2), and $\beta = 0.5$ (3).

SYNCHROTRON RADIATION RESEARCH 49

CASE I : $\frac{v}{c} \ll 1$

ELECTRON ORBIT

ACCELERATION

ELECTRON ORBIT

ACCELERATION

} ARC VIEWED BY OBSERVER

$\theta_v \approx \frac{mc^2}{E}$

CASE II : $\frac{v}{c} \approx 1$

Figure 3 Pattern of radiation emitted by electrons in circular motion. Case I: non-relativistic electrons, $v/c \ll 1$. Case II: relativistic electrons, $v/c \approx 1$.

3

Sources: X-Ray Data Booklet, LBNL; "Spectra and Optics of SR", BNL

LBNL/PUB-490 Rev. 3

**Center for X-Ray Optics
and
Advanced Light Source**

X-RAY DATA BOOKLET

Albert Thompson   Ingolf Lindau
David Attwood   Yanwei Liu
Eric Gullikson   Piero Pianetta
Malcolm Howells   Arthur Robinson
Kwang-Je Kim   James Scofield
Janos Kirz   James Underwood
Jeffrey Kortright   Gwyn Williams
          Herman Winick

October 2009

Lawrence Berkeley National Laboratory
University of California
Berkeley, CA 94720

This work was supported in part by the U.S. Department
of Energy under Contract No. DE-AC02-05CH11231

SECTION 1

BNL 50522
(Particle Accelerators and
High-Voltage Machines - TID 4500)

SPECTRA AND
OPTICS OF SYNCHROTRON RADIATION

G.K. Green

April 15, 1976

ACCELERATOR DEPARTMENT
BROOKHAVEN NATIONAL LABORATORY
ASSOCIATED UNIVERSITIES, INC.
UPTON, NEW YORK 11973
under contract No. E(30-1)-16 with the
UNITED STATES ENERGY RESEARCH AND DEVELOPMENT ADMINISTRATION

4

Sources: X-Ray Data Booklet, LBNL; "Spectra and Optics of SR", BNL

LBNL/PUB-490 Rev. 3

Center for X-Ray Optics
and
Advanced Light Source

X-RAY DATA BOOKLET

Albert Thompson	Ingolf Lindau
David Attwood	Yanwei Liu
Eric Gullikson	Piero Pianetta
Malcolm Howells	Arthur Robinson
Kwang-Je Kim	James Scofield
Janos Kirz	James Underwood
Jeffrey Kortright	Gwyn Williams
	Herman Winick

October 2009

Lawrence Berkeley National Laboratory
University of California
Berkeley, CA 94720

This work was supported in part by the U.S. Department of Energy under Contract No. DE-AC03-00SF-00098
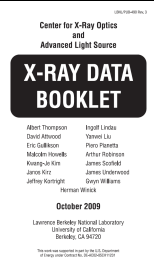
SECTION 2

SYNCHROTRON RADIATION

2.1A CHARACTERISTICS OF SYNCHROTRON RADIATION

Kwang-Je Kim

Synchrotron radiation occurs when a charge moving at relativistic speeds follows a curved trajectory. In this section, formulas and supporting graphs are used to quantitatively describe characteristics of this radiation for the cases of circular motion (bending magnets) and sinusoidal motion (periodic magnetic structures).

We will first discuss the ideal case, where the effects due to the angular divergence and the finite size of the electron beam—the emittance effects—can be neglected.

A. BENDING MAGNETS

The angular distribution of radiation emitted by electrons moving through a bending magnet with a circular trajectory in the horizontal plane is given by

$$\frac{d^2 \mathcal{F}_B(\omega)}{d\theta d\psi} = \frac{3\alpha}{4\pi^2} \gamma^2 \frac{\Delta\omega}{\omega} \frac{I}{e} y^2 (1+X^2)^2 \times \left[K_{2/3}^2(\xi) + \frac{X^2}{1+X^2} K_{1/3}^2(\xi) \right], \tag{1}$$

2-2

where

$\mathcal{F}_B$ = photon flux (number of photons per second)
θ = observation angle in the horizontal plane
ψ = observation angle in the vertical plane
α = fine-structure constant
γ = electron energy/$m_e c^2$ (m_e = electron mass, c = velocity of light)
ω = angular frequency of photon ($\varepsilon = \hbar\omega$ = energy of photon)
I = beam current
e = electron charge = 1.602×10^{-19} coulomb
y = $\omega/\omega_c = \varepsilon/\varepsilon_c$
ω_c = critical frequency, defined as the frequency that divides the emitted power into equal halves, = $3\gamma^3 c/2\rho$
ρ = radius of instantaneous curvature of the electron trajectory (in practical units, $\rho[m] = 3.3\ E[GeV]/B[T]$)
E = electron beam energy
B = magnetic field strength
ε_c = $\hbar\omega_c$ (in practical units, $\varepsilon_c[keV] = 0.665\ E^2[GeV]\ B[T]$)
X = $\gamma\psi$
ξ = $y(1+X^2)^{3/2}/2$

The subscripted K's are modified Bessel functions of the second kind. In the horizontal direction ($\psi = 0$), Eq. (1) becomes

$$\left. \frac{d^2 \mathcal{F}_B}{d\theta d\psi} \right|_{\psi=0} = \frac{3\alpha}{4\pi^2} \gamma^2 \frac{\Delta\omega}{\omega} \frac{I}{e} H_2(y), \tag{2}$$

where

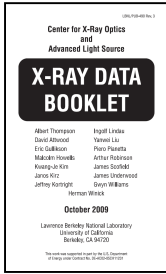$$H_2(y) = y^2 K_{2/3}^2(y/2) . \tag{3}$$

In practical units [photons·s⁻¹·mr⁻²·(0.1% bandwidth)⁻¹],

$$\left. \frac{d^2 \mathcal{F}_B}{d\theta d\psi} \right|_{\psi=0} = 1.327 \times 10^{13} E^2[GeV]\ I[A] H_2(y).$$

The function $H_2(y)$ is shown in Fig. 2-1.

From now on, θ is the horizontal observation angle, and Ψ the vertical one, with respect to the plane of the orbit

5

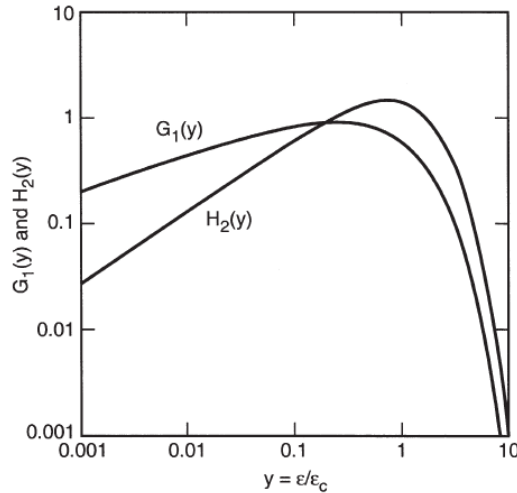# Sources: X-Ray Data Booklet, LBNL; "Spectra and Optics of SR", BNL

Center for X-Ray Optics and Advanced Light Source

X-RAY DATA BOOKLET

Albert Thompson · Ingolf Lindau
David Attwood · Yanwei Liu
Eric Gullikson · Piero Pianetta
Malcolm Howells · Arthur Robinson
Kwang-Je Kim · James Scofield
Janos Kirz · James Underwood
Jeffrey Kortright · Gwyn Williams
Herman Winick

October 2009

Lawrence Berkeley National Laboratory
University of California
Berkeley, CA 94720

2-3

Fig. 2-1. The functions $G_1(y)$ and $H_2(y)$, where y is the ratio of photon energy to critical photon energy.

The distribution integrated over ψ is given by

$$\frac{d\mathcal{F}_B}{d\theta} = \frac{\sqrt{3}}{2\pi}\alpha\gamma\frac{\Delta\omega}{\omega}\frac{I}{e}G_1(y),\qquad(4)$$

where

$$G_1(y) = y\int_y^\infty K_{5/3}(y')dy'\qquad.\qquad(5)$$

In practical units [photons·s⁻¹·mr⁻¹·(0.1% bandwidth)⁻¹],

$$\frac{d\mathcal{F}_B}{d\theta} = 2.457\times10^{13}\,E[\text{GeV}]I[\text{A}]G_1(y).$$

The function $G_1(y)$ is also plotted in Fig. 2-1.

Radiation from a bending magnet is linearly polarized when observed in the bending plane. Out of this plane, the polarization is elliptical and can be decomposed into its horizontal and vertical components. The first

---

2-4

and second terms in the last bracket of Eq. (1) correspond, respectively, to the intensity of the horizontally and vertically polarized radiation. Figure 2-2 gives the normalized intensities of these two components, as functions of emission angle, for different energies. The square root of the ratio of these intensities is the ratio of the major and minor axes of the polarization ellipse. The sense of the electric field rotation reverses as the vertical observation angle changes from positive to negative.

Synchrotron radiation occurs in a narrow cone of nominal angular width $\sim 1/\gamma$. To provide a more specific measure of this angular width, in terms of electron and photon energies, it is convenient to introduce the effective rms half-angle σ_ψ as follows:

$$\frac{d\mathcal{F}_B}{d\theta}\frac{d^2\mathcal{F}_B}{d\theta d\psi}\bigg|_{\psi=0} = \sqrt{2\pi}\,\sigma_\psi,\qquad(6)$$
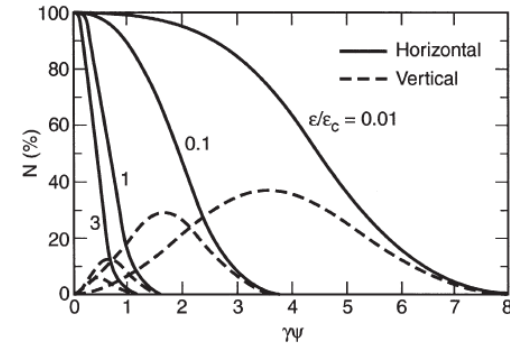
Fig. 2-2. Normalized intensities of horizontal and vertical polarization components, as functions of the vertical observation angle ψ, for different photon energies. (Adapted from Ref. 1.)

- 7/8 of total power into Hor. Polarization;
- 1/8 into Vertical Polarization

Sources: X-Ray Data Booklet, LBNL; "Spectra and Optics of SR", BNL; V. Baglin (IPAC-11); Author: SYNRAD+ simulation;
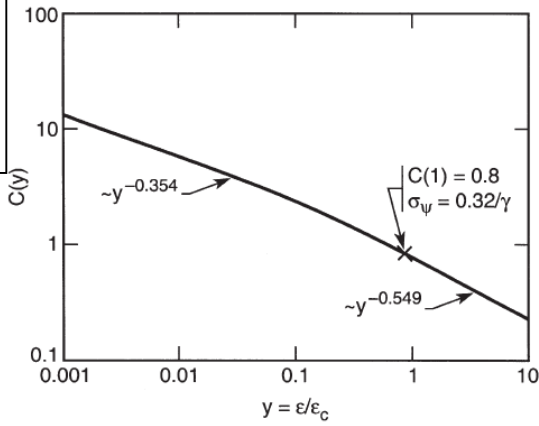

Fig. 2-3. The function C(y). The limiting slopes, for $\varepsilon/\varepsilon_c \ll 1$ and $\varepsilon/\varepsilon_c \gg 1$, are indicated.

where σ_ψ is given by

$$\sigma_\psi = \frac{2}{\gamma\sqrt{2\pi}} C(y) = 0.408 \frac{C(y)[\text{mr}]}{E[\text{GeV}]} \quad . \quad (7)$$

The function C(y) is plotted in Fig. 2-3. In terms of σ_ψ, Eq. (2) may now be rewritten as

$$\left.\frac{d^2\mathcal{F}_B}{d\theta d\psi}\right|_{\psi=0} = \frac{d\mathcal{F}_B}{d\theta}\frac{1}{\sigma_\psi\sqrt{2\pi}}. \quad (2a)$$
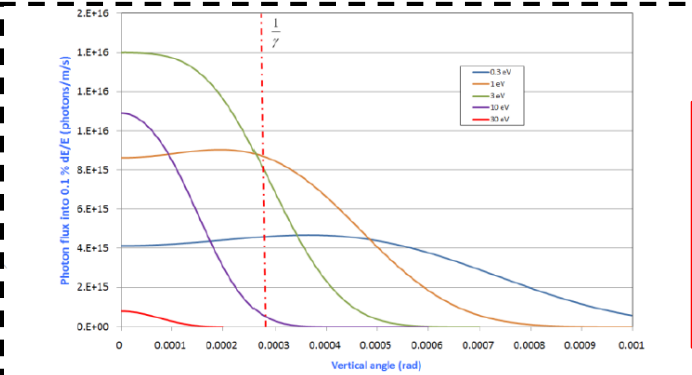
Figure 2: Photon flux distribution in the vertical angle at 3.5 TeV.

Vertical Distribution of SR Power and Flux (Dipole)

SR_{power} SR_{flux}

$\varepsilon > 10$ eV

$\gamma \cdot \Psi$ (mrad)

Equivalent Rectangle

MC Data Fitted to y=exp(-x²/2σ²) { σ=1.234 ; σ=0.605 }
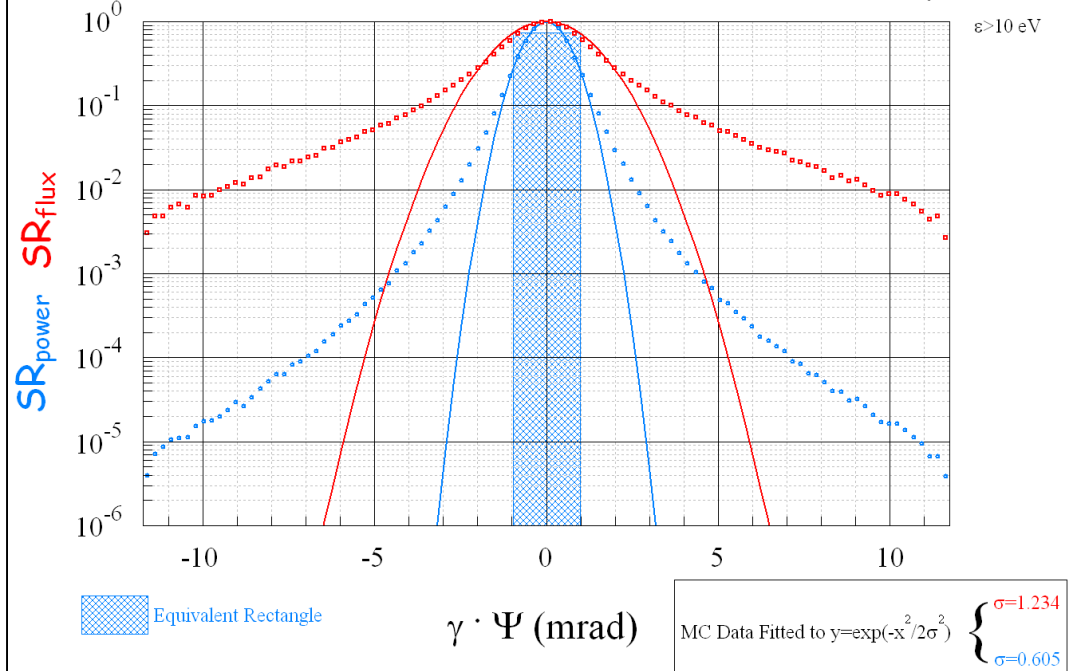
<- LHC ->IPAC-11 Conference paper, V. Baglin et al.;

MC simulation, SYNRAD+ -> author, with parabolic fit within |γΨ|<1 range

Vertical Distribution of SR Power and Flux (Dipole)

SR_{power}, SR_{flux} (A.U.)

$\varepsilon > 10$ eV

$\gamma \cdot \Psi$ (mrad)

Equivalent Rectangle

MC Data Fitted to y=exp(-(x²)/2σ²) { σ=1.234 ; σ=0.605 }

7
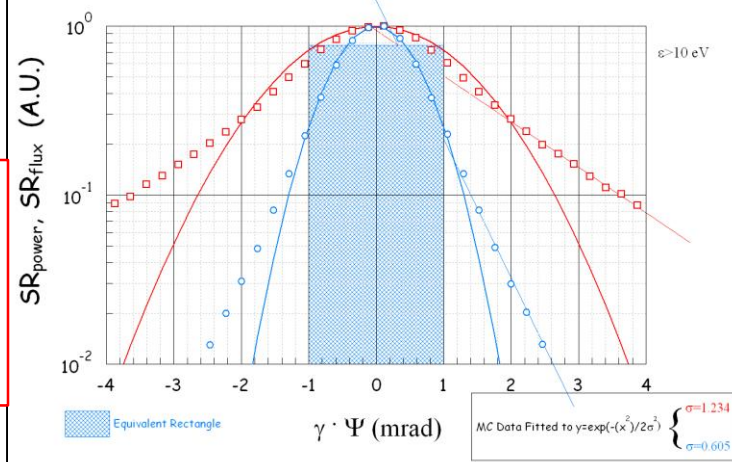
Author: Montecarlo Simulation with SYNRAD+

Distribution of the Synchrotron Radiation Fan vs Vertical Angle

Dashed: Flux
Solid: Power

Computed with SYNRAD+

Vertical Distribution of SR Power and Flux (Dipole)

$\varepsilon > 10$ eV

SR_{power} SR_{flux}

$\gamma \cdot \Psi$ (mrad)

Equivalent Rectangle

MC Data Fitted to y=exp(-x²/2σ²) $\begin{cases} \sigma=1.234 \\ \sigma=0.605 \end{cases}$
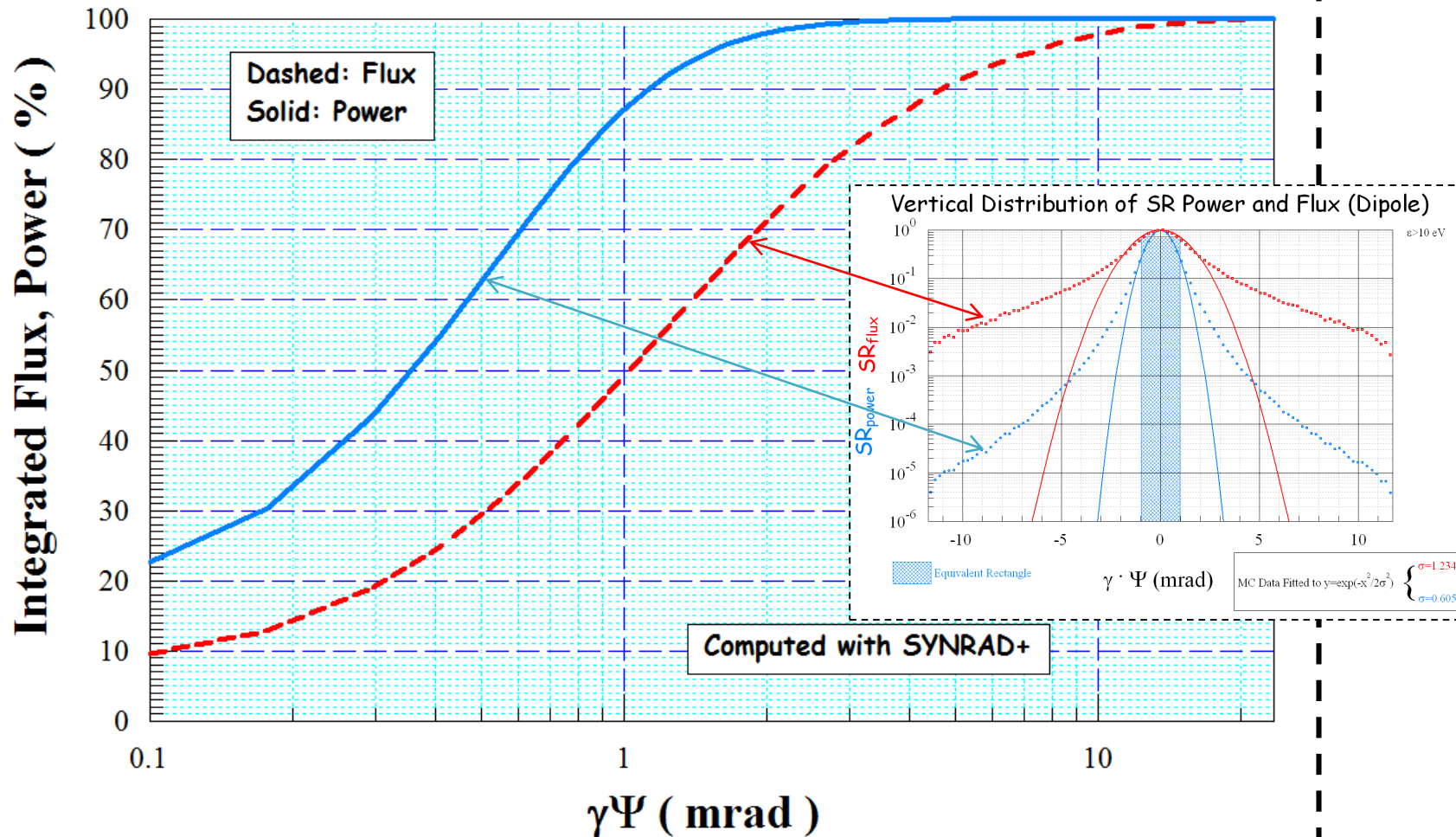
Message: there are MANY photons which are generated at very large angles!!

Author: Montecarlo Simulation with SYNRAD+
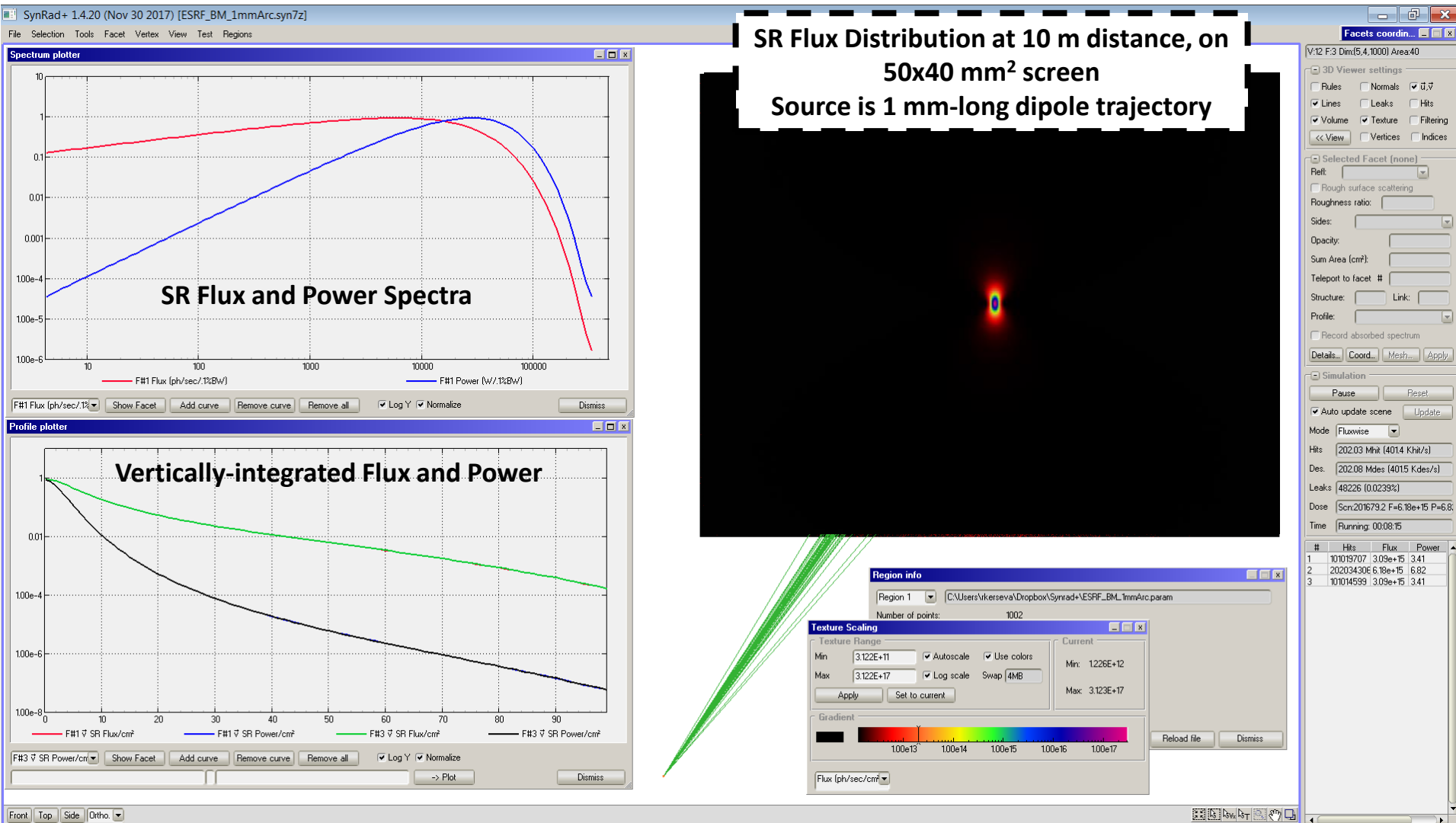
Flux distribution above:
- **View 1: log scale (~ 6 orders of magnitude);**
- **View 2: linear scale;**

8

Sources: X-Ray Data Booklet, LBNL; "Spectra and Optics of SR", BNL
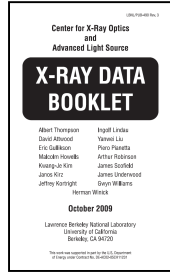
$$\gamma = \frac{1}{\sqrt{1 - \dfrac{v^2}{c^2}}}$$
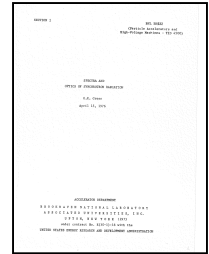
Practical Formulae, as a function of rel.factor γ:

Integrated Photon Flux, F : $F = 4.1289E + 14 \cdot \gamma \cdot I(mA) \cdot k_F$ (ph/s/mA)

Integrated Photon Power, P: $P = 6.0344E - 12 \cdot \dfrac{\gamma^4}{\rho(m)} \cdot I(mA) \cdot k_P$ (W/mA)

Critical Energy, e_{crit} : $e_{crit} = 2.9596E - 7 \cdot \dfrac{\gamma^3}{\rho(m)}$ (eV)

k_f, k_p = fraction of photons with energies above a given <u>threshold</u>;

Source: "Efficient computation of synchrotron radiation spectrum",
H.H. Umstatter, CERN/PS/SM/81-13, 1981

How can spectra and fluxes be calculated efficiently and fast?

- Several numerical algorithms have been developed during the years:
- This one, is particularly fast:

f) The highest speed is obtained if one computes directly $\int K_{5/3}$ by a Chebyshev series instead of separate computation of $K_{2/3}$ and $\int K_{1/3}$. Since it is not known whether Chebyshev expansion coefficients of $\int K_{5/3}$ exist in the literature they are given in the following listing of subroutine SYNRAD, rounded to 10 digits after the decimal point. Coefficients of 19 – 20 digit precision are given in the following table. They have been computed by linear combination of Luke's coefficients for $K_{2/3}$ and $\int K_{1/3}$. SYNRAD calls no external subroutine and uses no array in order to gain more speed. It is about 400 times faster than method a. On the IBM it evaluates $\int K_{5/3}$ in $7.6 \cdot 10^{-5}$ sec. on the CDC 7600 in $2.6 \cdot 10^{-5}$ sec. (i.e. 38600 values in 1 sec. computing time).

EUROPEAN ORGANISATION FOR NUCLEAR RESEARCH

CERN/PS/SM/81-13
10.3.1981.

/1mg

EFFICIENT COMPUTATION OF SYNCHROTRON RADIATION SPECTRUM

H.H. Umstätter
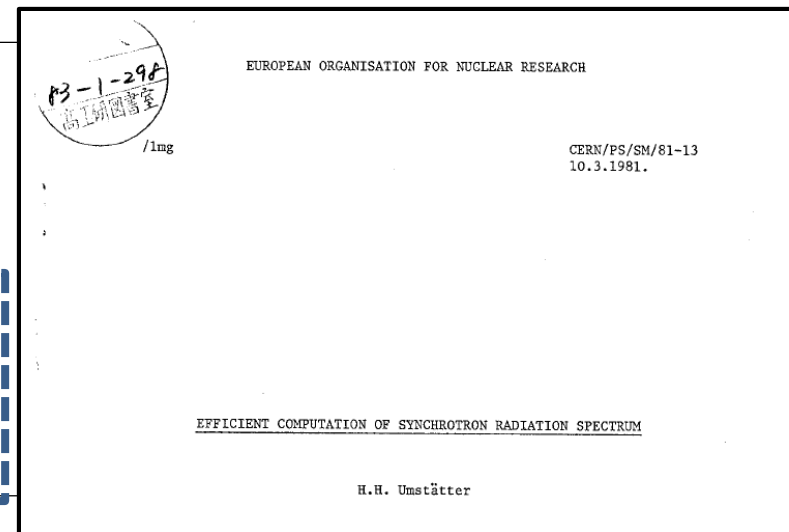
- Note: compared to the CDC 7600 supercomputer of the early 80's, the same code running on just *one* core of a modern multi-core CPU looks like a rocket: 1.6M values/sec *vs* 38600 values/sec, an improvement of > 40:

This means that today <u>**montecarlo simulations of SR are computationally-affordable even on laptop and desktop computers.**</u>

Source: "Efficient computation of synchrotron radiation spectrum",
H.H. Umstatter, CERN/PS/SM/81-13, 10/03/1981

The FORTRAN code: ->

```
      FUNCTION SYNRAD(X)
C     COMPUTES INTEGRAL X TO INF.OF MOD.BESSEL FUNCTION K,ORDER 5/3
      IF(X.LT.6.) GO TO 1
      Z=20./X-2.
      A=                      +.0000000001
      B=      Z*A             -.0000000004
      A=      Z*B-A           +.0000000020
      B=      Z*A-B           -.0000000110
      A=      Z*B-A           +.0000000642
      B=      Z*A-B           -.0000004076
      A=      Z*B-A           +.0000028754
      B=      Z*A-B           -.0000232125
      A=      Z*B-A           +.0002250532
      B=      Z*A-B           -.0028763680
      A=      Z*B-A           +.0623959136
      P=.5*Z*A-B             +1.0655239080
      SYNRAD=P*SQRT(1.5707963268/X)/EXP(X)
      RETURN
    1 Z=X**2/16.-2.
      A=                      .0000000001
      B=      Z*A     +       .0000000023
      A=      Z*B-A+          .0000000813
      B=      Z*A-B+          .0000024575
      A=      Z*B-A+          .0000618126
      B=      Z*A-B+          .0012706638
      A=      Z*B-A+          .0209121680
      B=      Z*A-B+          .2688034606
      A=      Z*B-A+         2.6190218379
      B=      Z*A-B+        18.6525089687
      A=      Z*B-A+        92.9523266592
      B=      Z*A-B+       308.1591941313
      A=      Z*B-A+       644.8697985824
      P=.5*Z*A-B+        414.5654364883
      A=                      .0000000012
      B=      Z*A     +       .0000000391
      A=      Z*B-A+          .0000011060
      B=      Z*A-B+          .0000258145
      A=      Z*B-A+          .0004876869
      B=      Z*A-B+          .0072845620
      A=      Z*B-A+          .0835793546
      B=      Z*A-B+          .7103136129
      A=      Z*B-A+         4.2678026127
      B=      Z*A-B+        17.0554078580
      A=      Z*B-A+        41.8390348678
      Q=.5*Z*A-B+        28.4178737436
      Y=X**0.66666666667
      SYNRAD=(P/Y-Q*Y-1.)*1.8137993642
      RETURN
      END
```

Calculation of…

$$G(x) = \int_x^\infty K_{\frac{5}{3}}(t)\,dt$$

… by means of a Chebyshev series expansion

CHEBYSHEV COEFFICIENTS FOR INTEGRAL OF $K_{\frac{5}{3}}(x)$.

$$0 \le x \le 8: \quad \int_x^\infty K_{\frac{5}{3}}(t)\,dt = \frac{\pi}{\sqrt{3}}\left(x^{-2/3} \sum_{n=0}^{\infty} A_-(n)\, \overline{T}_n(\xi) - 1 - x^{+2/3} \sum_{n=0}^{\infty} A_+(n)\, \overline{T}_n(\xi) \right)$$

$$\xi = 2\left(\frac{x}{8}\right)^2 - 1$$

11

Sources: LHC ->IPAC-11 Conference paper; ESRF -> "Blue Book"

k_f, k_p = fraction of photons with energies above given threshold:

- It has been observed that only photons whose energy is above a given <u>threshold</u> are capable of generating <u>gas desorption</u> (see P. Chiggiato's lecture, previous JUAS).

- In literature, it is often the value of E_{thr} ~ **4eV** which is chosen (work function)

- During energy ramping of the LHC from 450 GeV (SPS extraction energy) to 3500 GeV, some vacuum gauges installed in the warm sections of the machine have indicated a <u>sudden rise around 2500 GeV</u>, as shown here below

12

Photon Flux Cut-Off vs Critical Energy

4 eV FLUX CUT-OFF %

2.5 TeV~ 97%

3.5 TeV~ 86%
4.0 TeV~ 80%

7.0 TeV~ 52%

16.5 TeV~ 23%
(@HE-LHC, 20 T magnets)

Fig.11 Percent of photons at all wavelengths greater than λ vs λ/λ_{crit}

("Spectra and Optics of SR", G.K. Green, BNL 50522, 1976)

$$\lambda/\lambda_c = e_{crit}/e$$
$$\lambda(e)(\mu m) = 1.239842/e(eV)$$

LHC Crit.Energy(eV) ---> 2.0   5.5 8.2   43.8   573.9

Critical Energy ESRF (eV):   20,504
CUT-OFF ~ 8%

13
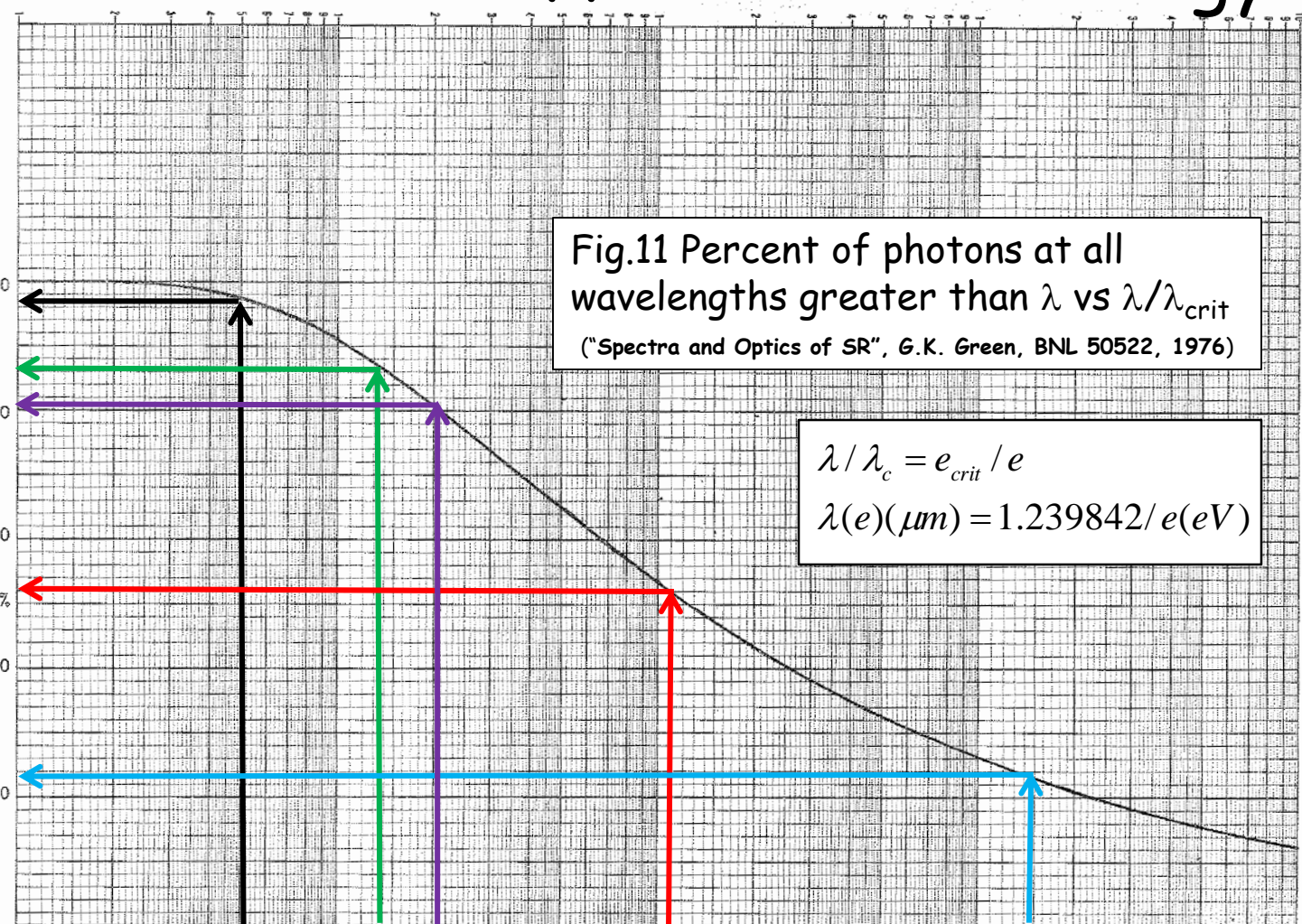
Machine Parameters:

Type	Energy(GeV)	BMField(T)	BMRadius(m)	Rel.Factor	E_{crit}(eV)
LHC: p-p collider	450~7000	0.54 ~ 8.33	2803.95	480 ~ 7460	0.012 ~ 43.8
ESRF: e⁻ light src.	6.0	0.86	23.366	11,740	20,504

Machine Parameters:

Type	Circumf.(m)	I_{nom}(mA)	Ph.Flux(ph/s/m)	Ph.Power(W/m)
LHC: p-p collider	26,658.9	584	6.56E+15 ~ 1.02E+17	1.1E-4 ~ 0.22
ESRF: e⁻ light src.	844.4	200	6.60E+18	6,687.0
				(**63,700** @SC Wavelength Shifter)

Case Study: Comparison Between LHC and ESRF Synchrotron Radiation Fluxes and Spectra

Sources: LHC ->IPAC-11 Conference paper   **ESRF -> "Blue Book" (unpublished)**

SYNCHROTRON RADIATION IN THE LHC VACUUM SYSTEM

V. Baglin, G. Bregliozzi, J.M. Jimenez, G. Lanza
CERN, Geneva, Switzerland

Abstract
CERN is currently operating the Large Hadron Collider (LHC) with 3.5 TeV per beam. At this energy level, when the protons trajectory is bent, the protons emit synchrotron radiation (SR) with a critical energy of 5.5 eV. Under operation, SR induced molecular desorption is routinely observed in the LHC arcs, long straight sections and experiments. This contribution recalls the SR parameters over the LHC ring for the present and nominal beam parameters. Vacuum observations during energy ramp, after accumulation of dose and along the LHC ring are discussed. Expected pressure profiles and long term behaviours of vacuum levels will be also addressed.

INTRODUCTION

The Large Hadron Collider (LHC), currently under operation at CERN, is designed to push further our understanding of particle physics [1]. This is the first proton storage ring which is producing a significant quantity of synchrotron radiation (SR) which affects the vacuum system. At 7 TeV per beam and with nominal beam current, the LHC photon flux will be about 3 times larger than LEP200, the previous CERN headlight machine operating with electrons and positrons. However, being a proton machine, the dissipated power by SR will be much lower than LEP200 *i.e.* 0.2 W/m against 1 kW/m. To achieve 7 TeV per beam in the 27 km circumference tunnel, the arc dipole field must equals 8.3 T. Thus, the superconducting technology is required to circulate a current of 11.85 kA in the Nb-Ti cables. These cables are cooled down to 1.9 K to increase further their performances.

The arc vacuum system is made of a cold bore held at 1.9 K housing a beam screen designed to intercept the beam induced heat load at higher temperature to minimise the cryogenic budget. Along each cell of 102 m long, the temperature of the beam screen is increasing from 5-8 K to 20 K. By design, the available cooling capacity to extract the dynamic heat load on the beam screen varies from 1.5 to 2 W/m per aperture. Under SR bombardment, desorption of hydrogen is stimulated. Consequently, the molecules are physisorbed and accumulated on the beam screen surface. In a closed system operating at 5 K, the growth of a monolayer of hydrogen leads to a saturated vapour pressure of about 10^{-4} mbar, a value by far too large for a storage ring. So, the beam screen is perforated by slots to provide pumping of the desorbed gas onto the cold bore. Figure 1 shows a picture of the LHC arc beam screen. The beam screen is made of non-magnetic copper plated stainless steel. Its transparency is ~ 4 %. Saw teeth are produced in the horizontal plane to perpendicularly

intercept the SR, minimising the forward reflectivity and photoelectron yield. Shields, designed to protect the cold bore by intercepting the electron moving along the vertical dipole field lines, are clipped onto the cooling capillaries.

Figure 1: the LHC beam screen.

Due to the present interconnection design, the LHC energy is limited to 3.5 TeV per beam before upgrade to nominal after the next long shutdown.

LHC PARAMETERS

When a charged particle is accelerated longitudinally or transversally it produces a radiation. For a relativistic particle, this radiation is highly peaked in the forward direction with $1/\gamma$ opening angle. In a synchrotron, the radiation is emitted tangentially to the orbit in the horizontal plane. The energy of the emitted photons varies from infra-red to gamma rays *i.e.* from meV to MeV. The radiation spectrum is characterised by the critical energy, ε_c, energy at which the SR photon spectrum is halved in two. About 90 % of the emitted photons have energy lower than the critical energy.

The SR main parameters can be computed from formulas, see *e.g.* [2]. Here, practical equations are given for protons beam at a given beam current, I and energy, E.

The critical energy is expressed by (1) with h, the plank constant, c, the speed of light, ρ, the bending radius and γ the relativistic factor.

$$\varepsilon_c = \frac{3}{2}\frac{hc}{2\pi}\frac{\gamma^3}{\rho} = 3.853510^{-7}\frac{E[GeV]^3}{\rho[m]} \quad (1)$$

The average power emitted by the beam per unit of length is given by (2) with e the elementary charge ε_o the vacuum permittivity and m_o the proton classical radius.

$$P_0[W/m] = \frac{e}{3\varepsilon_0(m_0c^2)^4}\frac{E^4}{2\pi\rho^2}I = 7.7910^{-12}\frac{E[GeV]^4}{2\pi\rho[m]}I[mA] \quad (2)$$

The photon flux, $\dot{\Gamma}$, is expressed by (3).

$$\dot{\Gamma} = \frac{5\sqrt{3}e}{12\,h}\frac{\gamma}{\varepsilon_0 c}\frac{\gamma}{\rho}I = 7.01710^{13}\frac{E[GeV]}{\rho[m]}I[mA] \quad (3)$$

Arc Magnets
The LHC arc lattice is of FODO type. The beams are circulating in two beam lines separated by 194 mm. Each of the dipole emits SR along its magnetic length (14.3 m).

07 Accelerator Technology

T14 Vacuum Technology

EDMS no 1168511

1563

SYNCHROTRON RADIATION POWER DISTRIBUTION IN THE ESRF STORAGE RING VACUUM CHAMBERS

* FAN DRAWINGS

* POWER DISTRIBUTION ON THE ABSORBERS

Update March 2004   B. OGIER - B. PLAN - L. ZHANG

LHC "beam screen":

Linear power density: 14 mW/m @ 3.5 TeV
222 mW/m @ 7.0 TeV

BEAM SCREEN AT 5→20 K
USING 2 COOLING CHANNELS

COLD BORE 1.9 K

HOLES
TO PROVIDE PUMPING BY THE
1.9K COLD BORE
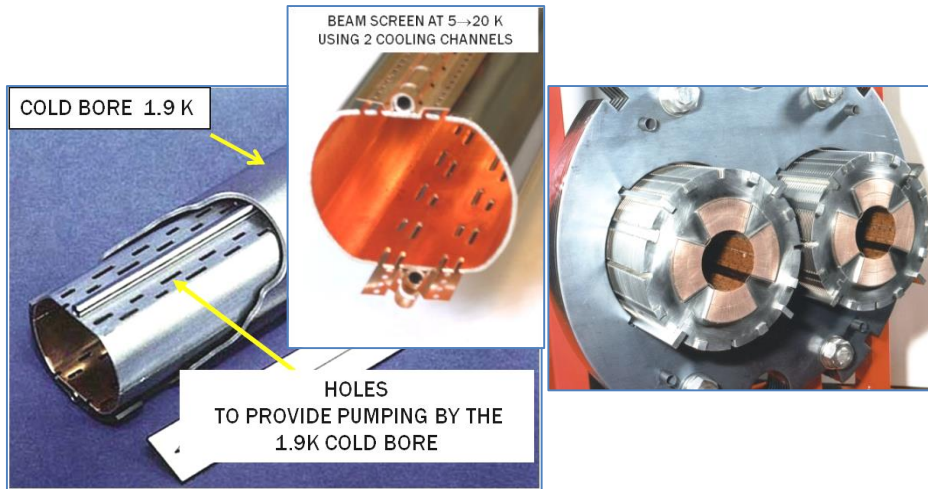
ESRF "crotch absorber":

Linear power density: 72 kW/m @ 6 GeV (pt.B)
Surface power dens.: 17.7 kW/cm^2 (pt. A)

from previous
dipole

to front-end /
beamline

A

B

20.150

80.81 ±0.1
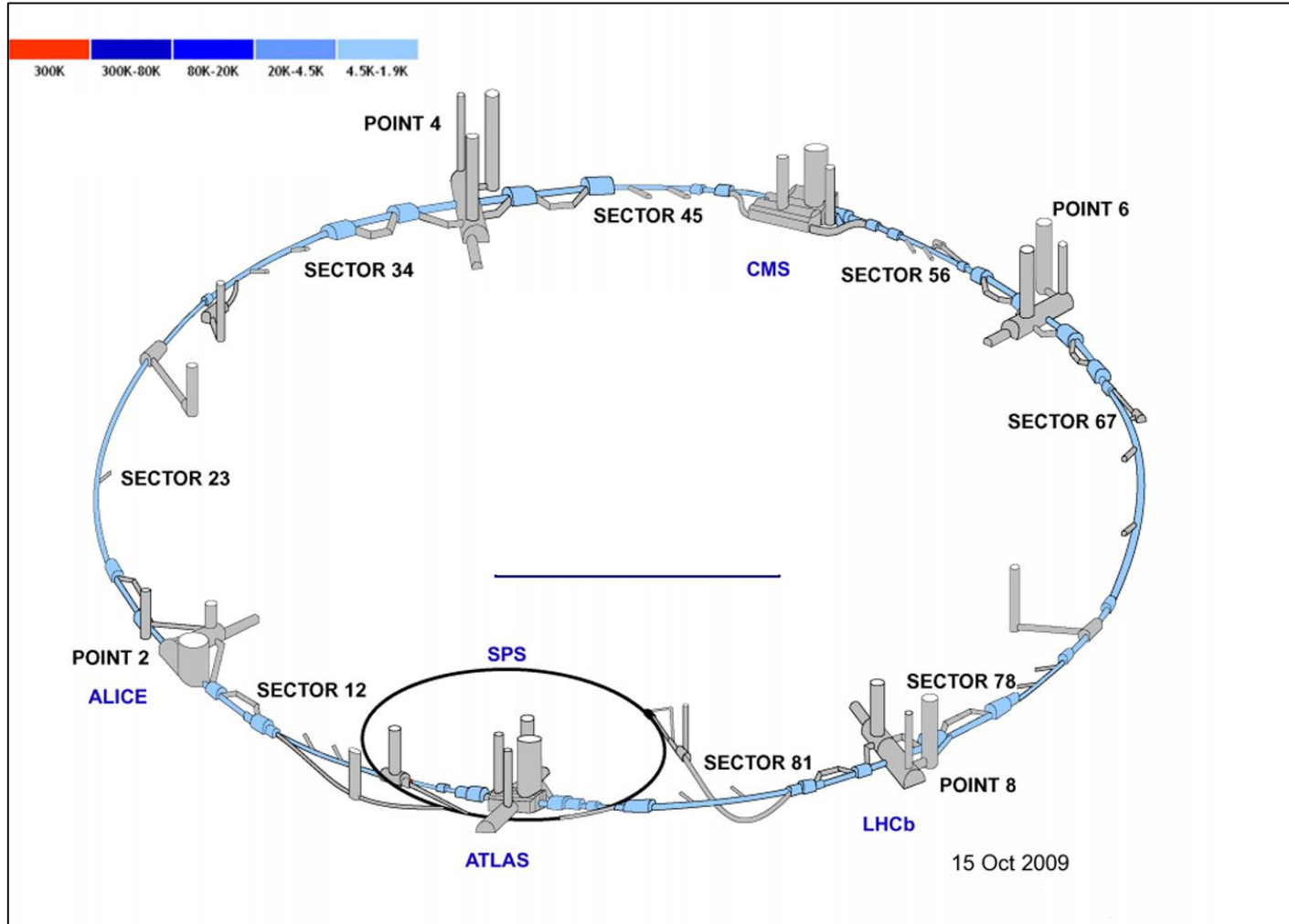
144.29 ±0.1

2.0 $^{0.0}_{-0.1}$

120.65±0.1
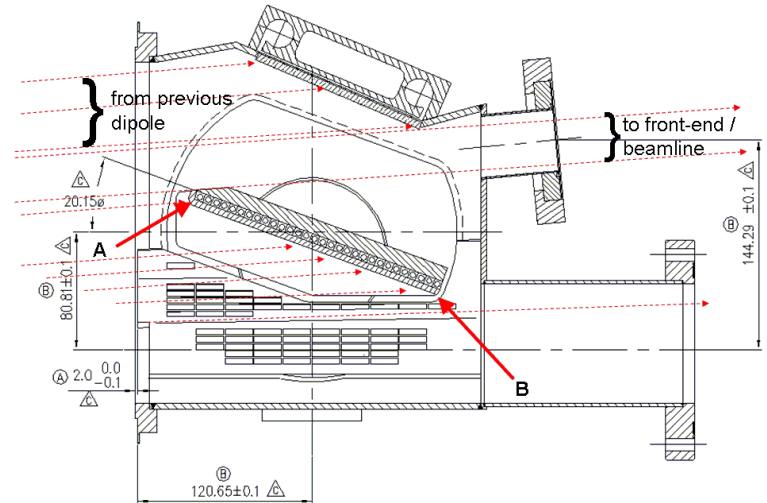
ESRF "quadrupole chamber": (most common shape)

Linear power density: 0.28 ~ 2.0 kW/m
Surface power dens.: 0.03 ~ 1.0 kW/cm^2
H_2O-cooled Cu absorber electron beam-
welded to 2mm-thick stainless steel sheet

ESRF STORAGE RING
QUADRUPOLE MAGNET VACUUM CHAMBER SECTION

PHOTON ABSORBER

74 mm

33 mm

Ø16.2

ELECTRON BEAM AXIS

MAGNET COIL

COOLING PIPES

MAGNET YOKE
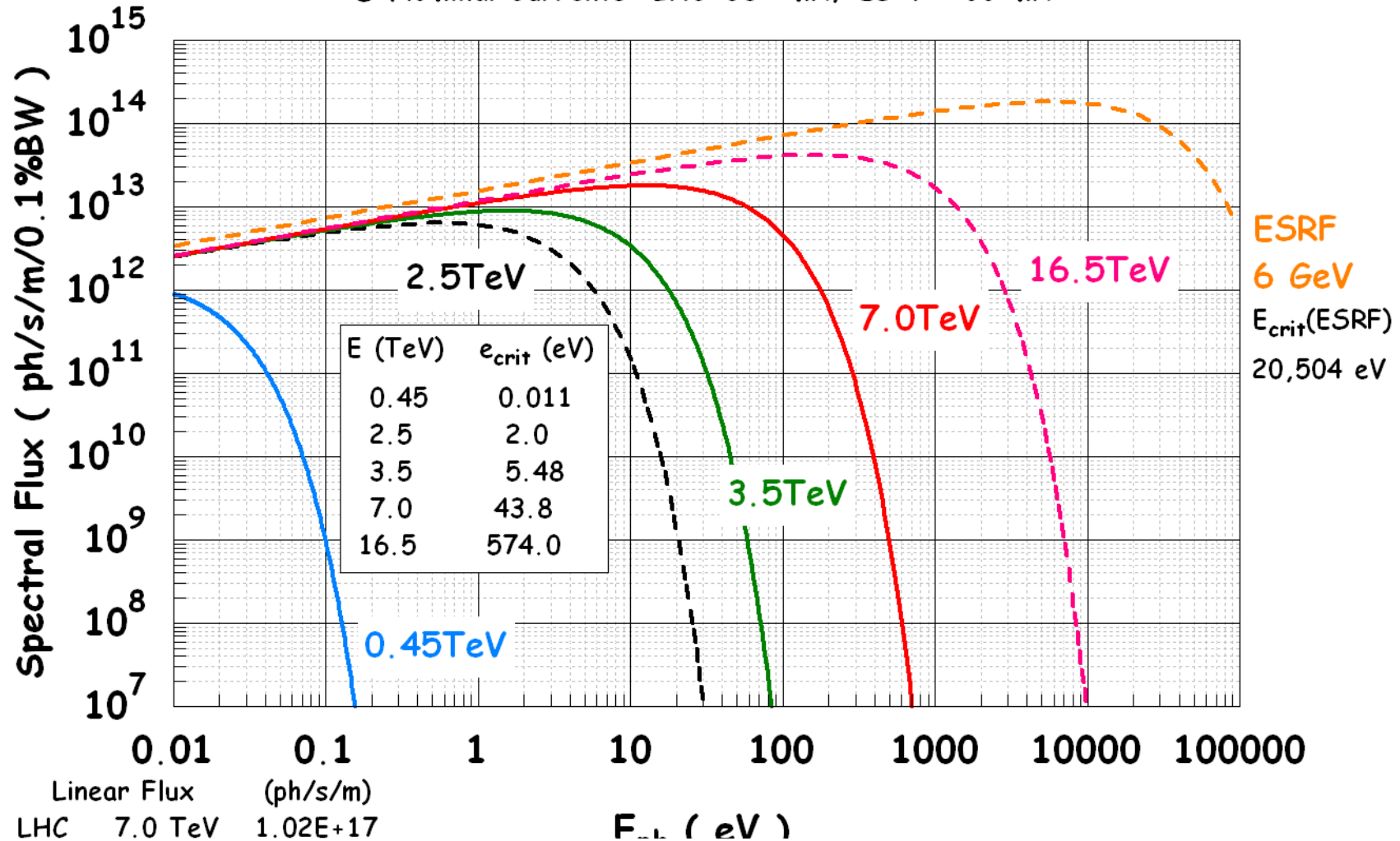
16
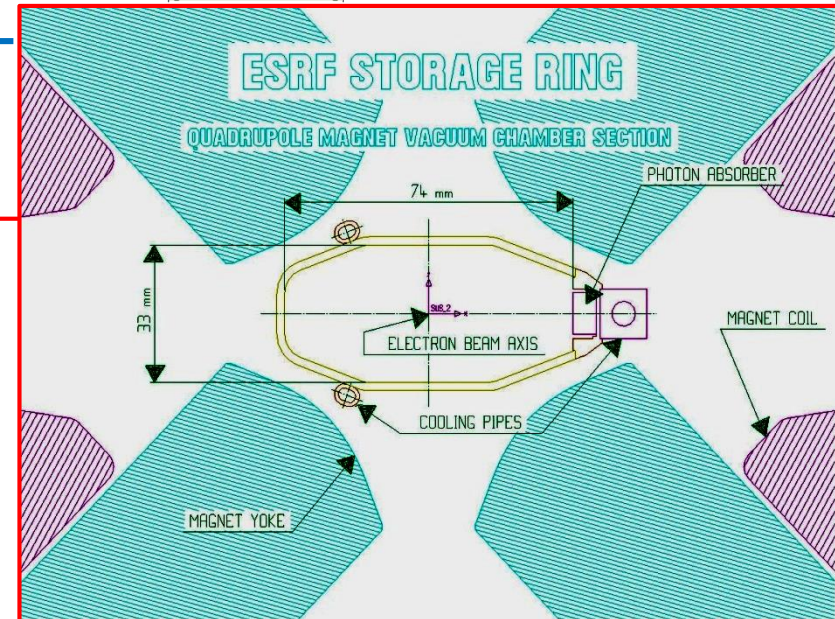
LHC p-p collider:

- **Beam Energy: 450 -> 7000 GeV** (injection from SPS to nominal ramp, now limited at 3500 GeV)
- **Beam Current: 584 mA** (nominal, i.e. 2808 bunches of 1.15E+11 p/each)
- **Circumference: 26,659 m**
- **All "arc sections" are cryogenically cooled at 1.9 °K**

17

Comparison of SR Flux Spectra: LHC vs ESRF
@ Nominal Currents: LHC=584 mA; ESRF=200 mA

E (TeV)	e_{crit} (eV)
0.45	0.011
2.5	2.0
3.5	5.48
7.0	43.8
16.5	574.0

ESRF
6 GeV

E_{crit}(ESRF)
20,504 eV

16.5TeV

7.0TeV

3.5TeV

2.5TeV

0.45TeV

Linear Flux	(ph/s/m)
LHC 7.0 TeV	1.02E+17
HE-LHC 16.5 TeV	2.41E+17
ESRF 6.0 GeV	6.60E+18

~ 20 T field... FCC Design Study (now 13.5 TeV, 16 T)

18

Comparison of SR Flux and Brilliance: LHC vs ESRF
@ Nominal Currents: LHC=584 mA; ESRF=200 mA
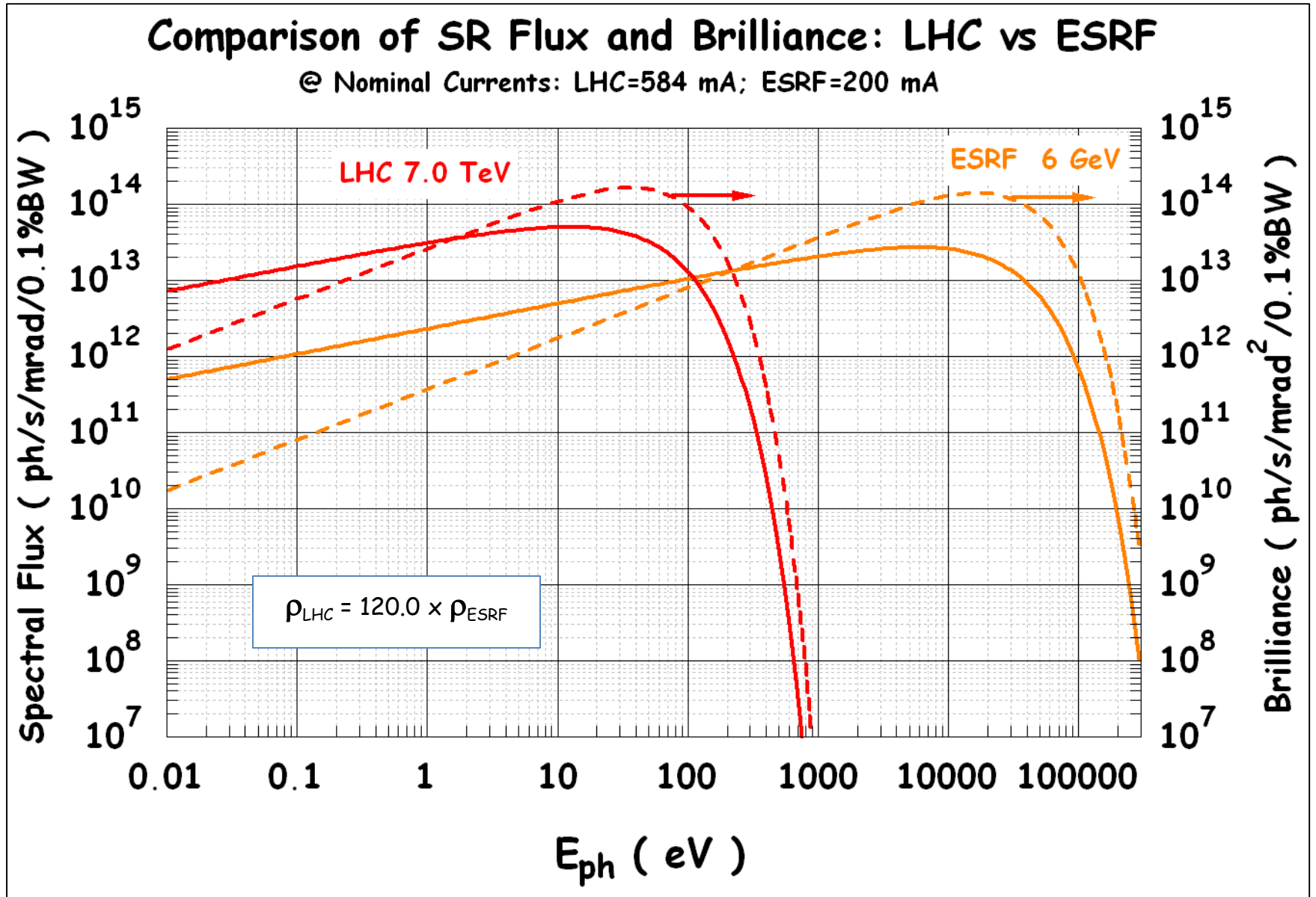
LHC Critical Energy vs Beam Energy
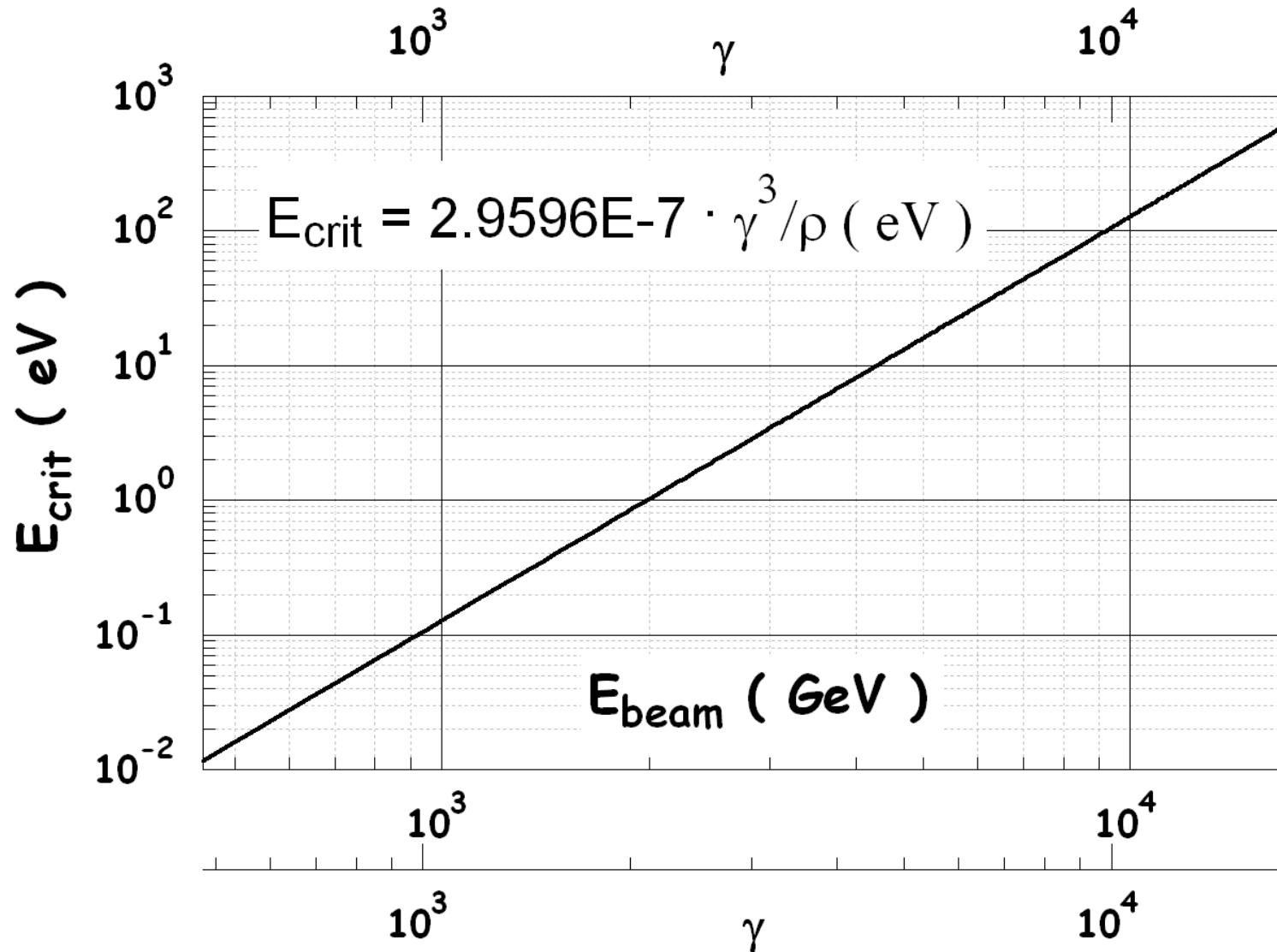
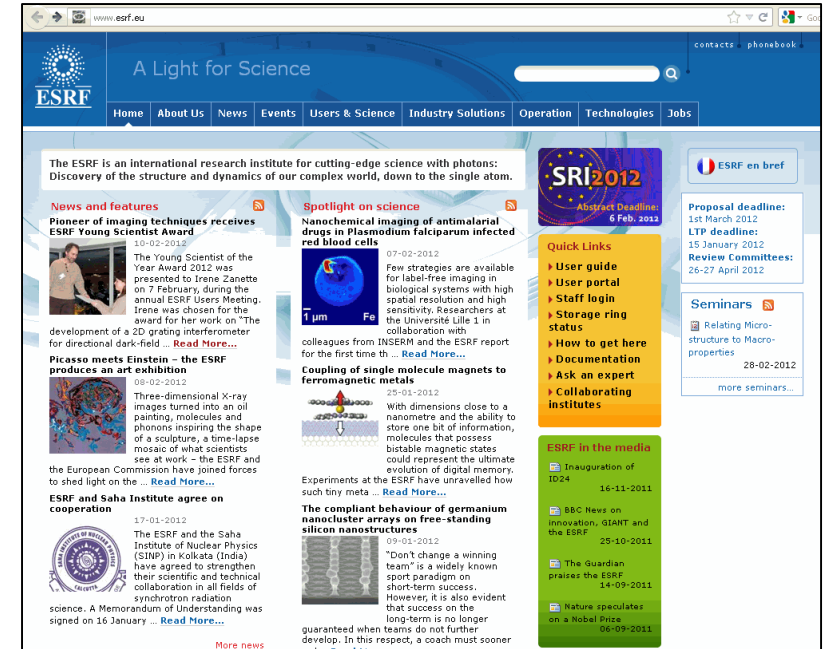$$E_{crit} = 2.9596E\text{-}7 \cdot \gamma^3/\rho \; (\, eV \,)$$

ESRF, 3rd generation synchrotron radiation light source:

- Beam Energy: 6 GeV
- Beam Current: 200 mA (uniform, 16-bunch, single-bunch, hybrid filling modes)
- Circumference: 845 m
- "Warm" machine, all magnets are resistive ones, at room temperature

ESRF, 3rd generation synchrotron radiation light source:

- Beam Energy: 6 GeV
- Beam Current: 200 mA (uniform, 16-bunch, single-bunch, hybrid filling modes)
- Circumference: 845 m
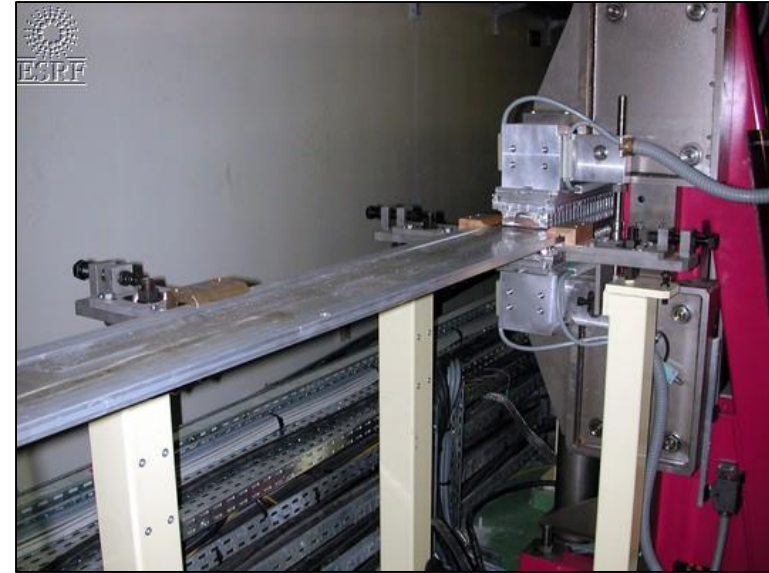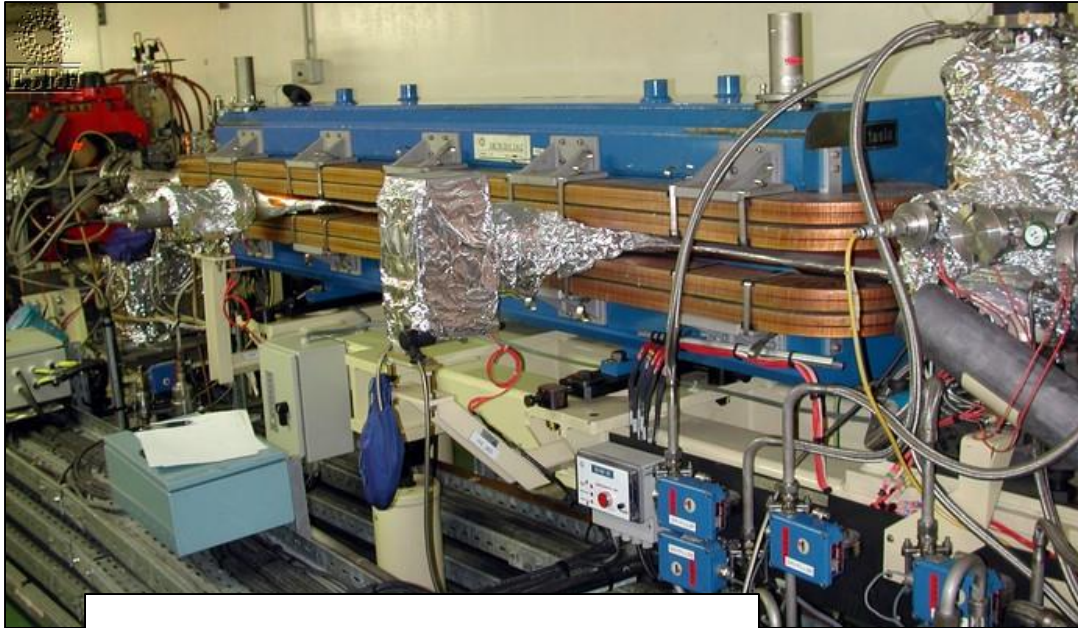- "Warm" machine, all magnets are resistive ones, at room temperature

- Insertion Device vacuum chamber (CV5073);
- Extruded Aluminum 6063 T6;
- Elliptical cross-section, 57x8 mm^2 axis, specific conductance ~1 l*m/s ONLY!
- NEG coated;
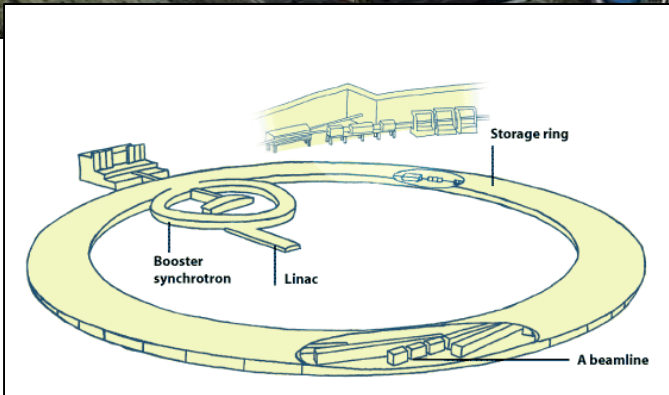
ESRF, 3rd generation synchrotron radiation light source:
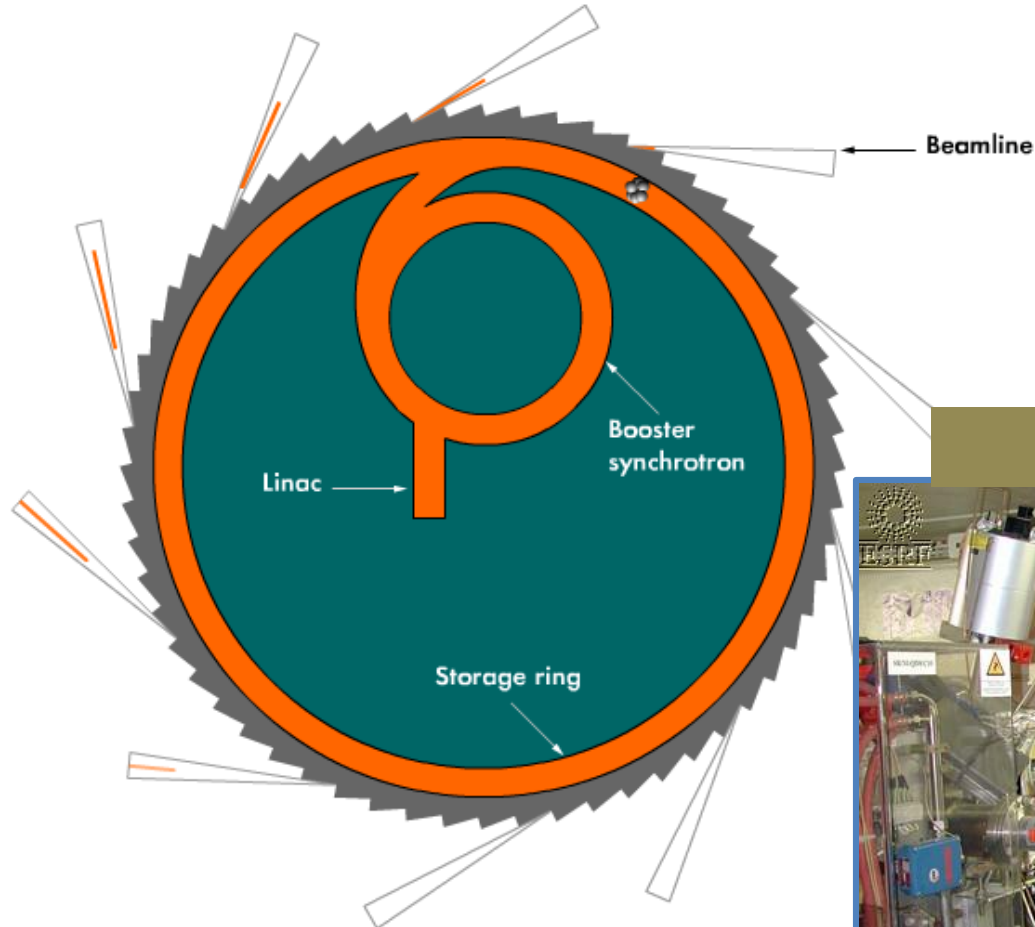
In-vacuum undulator

ESRF, 3rd generation synchrotron radiation light source:
Careful and detailed SR ray-tracing is mandatory!

ESRF

**SYNCHROTRON RADIATION
POWER DISTRIBUTION
IN THE ESRF STORAGE RING
VACUUM CHAMBERS**

* FAN DRAWINGS

* POWER DISTRIBUTION ON THE ABSORBERS

Update March 2004   B. OGIER - B. PLAN - L. ZHANG

-CONTENTS-

ESRF, 3rd generation synchrotron radiation light source:

Introduction

The basic synchrotron radiation sources are the bending magnets, which cover 2π radian angle. At the ESRF a major part of this synchrotron radiation is removed by water cooled heater absorbers installed inside the vacuum chambers of the Storage Ring. The power distribution on the absorbers is a basic data for the design of the vacuum chambers as well as the absorbers.

Additional sources of synchrotron radiation are Insertion Devices (ID's) placed in the straight section, between two successive bending magnets. At the ESRF the synchrotron radiation from the insertion devices has, in most cases, a very small horizontal opening angle so that it does not touch any components of the Storage Ring.

This document is intended to give out the power density and the spot size of the synchrotron radiation on all the absorbers of the ESRF Storage Ring vacuum chambers. Only the synchrotron radiation from bending magnets has been considered.

Basic Formula

The synchrotron radiation from a bending magnet in the ESRF has a much smaller vertical size and divergent angle than the horizontal ones. This synchrotron radiation can be considered as a horizontal divergent blade. The power distribution is then described by the angular power density which is defined by the power per unit angle in the horizontal plane, and a vertical Gaussian height.

The angular power density P_θ is given by

$$P_\theta = 4.224 \ B \ E^3 \ I \qquad (1)$$

where E : electron beam energy, in GeV
I : electron beam current intensity, in A
B : magnet field intensity of the bending magnet, in T
P_θ : angular power density in horizontal plane, in W/mrad

In the case of the ESRF, E = 6 GeV, I = 200 mA = 0.2 A, (nominal values)

- for the standard bending magnet B = 0.857 T,
$$P_\theta = 156.38 \ \text{W/mrad}$$
- for the soft end magnet B = 0.40 T,
$$P_\theta = 72.99 \ \text{W/mrad}$$

The linear power density P_l on the absorber is then

$$P_l = P_\theta \ \sin(\beta)/d \qquad (2)$$

where d is the distance between the source point and the absorber, in meter, β the incident angle of photon beam on the absorber (see Figure 1), P_l in W/mm.

The photon beam size on an absorber is characterised by the vertical Gaussian height σ (mm) which is calculated by

$$\sigma = \sqrt{\sigma_0^2 + (\sigma' d)^2 + (d/\gamma)^2} = \sqrt{\sigma_0^2 + (\sigma'' d)^2} \qquad (3)$$

where σ_0 : vertical standard deviation of the e-beam at source point (mm)
σ' : vertical angular standard deviation of the e-beam at source point (mrad)
σ'' : total effective vertical angular standard deviation at source point (mrad)
d : distance between source point and the absorber (m)
γ : = 1957 E (GeV)

For a coupling factor of 1% and a vertical emittance $\varepsilon_z = 4 \ 10^{-11}$ m.rad in the case of the ESRF,

$$\sigma_0 = 37 \ \mu m$$
$$\sigma' = 1.07 \ \mu rad$$
$$\gamma = 1.174 \ 10^4$$
$$\sigma'' = \sqrt{\sigma'^2 + 1/\gamma^2} = 85.2 \ \mu rad$$

ESRF, 3rd generation synchrotron radiation light source:

The surface power density on the absorber P_a is given by

$$P_a(z) = P_a \exp(-\frac{z^2}{2\sigma^2}) \qquad (4)$$

with peak power density per unit surface area :

$$P_a = \frac{P_l}{\sqrt{2\pi}\sigma} \qquad (5)$$

Once the distance d between the source point and the absorber is defined as well as the incidence angle β of the synchrotron radiation on the absorber, the power densities P_l, P_a and spot size on the absorber can be calculated by equations (2)-(5).
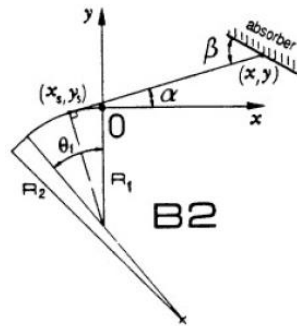
Geometrical calculation

There are two types of dipole bending magnets per cell in the ESRF storage ring :

1) with downstream soft end B1
2) with upstream soft end B2
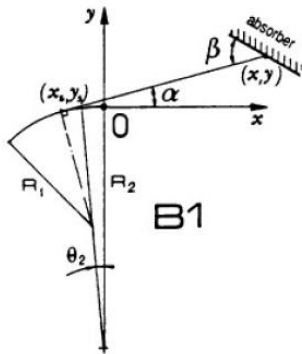
case 1 : dipole magnet B1

case 2 : dipole magnet B2

Figure 1 : Co-ordinate systems

The co-ordinate systems concerning the two types of dipole magnets are shown in Figure 1. The origin of the co-ordinate system is always at the exit of the magnets, the axis-x is parallel to the electron beam in the straight section. The absorber is defined by a certain number of key points and inclined angles $\gamma = \alpha + \beta$ of surface to the axis-x (or to the electron beam trajectory in the straight section).

It is easy to give out the co-ordinates of a point on the absorber (x, y) and the angle γ. The associated source point (x_s, y_s) and the angle α between the photon beam and the electron beam (see Figure 1) can be calculated from the co-ordinates (x, y) and the geometrical parameters of the bending magnets.

Case 1 : dipole magnet B1 :

  1) $\alpha > \theta_2$: source point on the main bending magnet (B1)

$$x_s = -R_1 \sin(\alpha) - (R_2 - R_1) \sin(\theta_2) \qquad (6a)$$
$$y_s = -R_2 + R_1 \cos(\alpha) + (R_2 - R_1) \cos(\theta_2) \qquad (6b)$$

  2) $\alpha < \theta_2$: source point on the soft end magnet

$$x_s = -R_2 \sin(\alpha) \qquad (7a)$$
$$y_s = -R_2 (1 - \cos(\alpha)) \qquad (7b)$$

Case 2 : dipole magnet B2 :

  3) $\alpha < \theta_1$: source point on the main bending magnet (B2)

$$x_s = -R_1 \sin(\alpha) \qquad (8a)$$
$$y_s = -R_1 (1 - \cos(\alpha)) \qquad (8b)$$

  4) $\alpha > \theta_1$: source point on the soft end magnet

$$x_s = -R_2 \sin(\alpha) + (R_2 - R_1) \sin(\theta_1) \qquad (9a)$$
$$y_s = -R_1 - (R_2 - R_1) \cos(\theta_1) + R_2 \cos(\alpha) \qquad (9b)$$

where R and θ are respectively the radius and the curvature angle of the magnet, index 1 for standard magnet and 2 for soft end magnet. At the ESRF,

ESRF, 3rd generation synchrotron radiation light source:

Two different radiuses on same dipole
-> Two different SR spectra

$R_1 = 23.366$ m

$R_2 = 50.036$ m

$\theta_1 = 92.324$ mrad

$\theta_2 = 5.85$ mrad

On the other hand :

$$\tan(\alpha) = \frac{y - y_s}{x - x_s} \qquad (10)$$

Substituting x_s, y_s given by the equations (6)-(9) in the equation (10), one gets an equation of α as below :

$$f(\alpha) = 0 \qquad (11)$$

For the example of 3) $\alpha < \theta_1$: source point on the main bending magnet (B2), $f(\alpha)$ is given by

$$f(\alpha) = \tan(\alpha)\,(x + R_1 \sin(\alpha)) - y - R_1\,(1 - \cos(\alpha))$$

Applying the Newton-Raphson method to the equation (11), we can calculate the value of angle α, as well as the incidence angle $\beta = \gamma - \alpha$. Then x_s, y_s are calculated by equations (6)-(9), and finally the distance d between the absorber and the source point :

$$d = \sqrt{(x - x_s)^2 + (y - y_s)^2} \qquad (12)$$

In summary, for any point on the absorber (x, y) with inclined angle γ,

1) distinguish the source type (1H, 2H, 1S, 2S)
2) combine one of Eq.(6)-(9) with the Eq.(10), solve the Eq.(11) to find the value of angle α, as well as the value of $\beta = \gamma - \alpha$
3) calculate co-ordinates of the source point (x_s, y_s) with Eq.(6)-(9)
4) calculate the distance d with Eq.(12)
5) calculate the photon beam height σ by Eq.(3)
6) calculate the linear power density P_l by Eq.(2)
7) calculate the surface power density P_a by Eq.(4)

The co-ordinate values (x, y), the angle α between the photon beams and electron beam, the incidence angle β, the photon beam size σ, the power densities P_l and P_a are given in the following tables for the key points of all the absorbers installed in the ESRF Storage Ring vacuum chambers. Once a beamline is installed, the beam port (a water cooled copper thermal absorber) is removed. The maximum power of dipole bending magnet to the beamline is then equal to what should be absorbed by the beam port.

There are 32 cells containing one dipole bending magnet B1 and one B2. The total power generated by the 2 dipole bending magnets in a cell, or the total power dissipated by the absorbers in one cell including the bending magnet synchrotron radiation power to the beamlines is 29.730 kW. The total dipole bending magnet synchrotron radiation power is then 951.36 kW, nearly 1 MW.

ESRF, 3rd generation synchrotron radiation light source:

Notation

The power distribution on the absorbers installed inside the vacuum chambers of the Storage Ring is presented as following.

(sample)

Pt n°	Src	Src n°	X mm	Y mm	α °	β °	σ mm	Pl W/mm	Pa W/mm2	Ptot W	CV n° / drawing n°
1		2	10 614	37.00	0.199	0.199	0.518	0.05	0.04		
2		2	12 728	37.00	0.166	0.166	0.620	0.04	0.02		
3	2H	2	12 846	37.34	0.166	9.628	0.625	2.03	1.29	130	CV 03 / 85.41.0073
4		2	12 848	37.00	0.165	9.627	0.626	2.02	1.29		
5		2	13 965	37.00	0.151	0.151	0.679	0.03	0.02		

Some symbols in the notation have been used in the previous sections. Here below is a summary of the notation.

Pt n°		number of points, marked in the drawings
Src		synchrotron radiation source type
Src n°		synchrotron radiation source number
	1H : dipole type 1,	n° =1
	2H : dipole type 2,	n° =2
	1S : soft end dipole type 1,	n° =0
	2S : soft end dipole type 2,	n° =3
X	(mm)	co-ordinate X, axis X parallel to the e-beam orbit
Y	(mm)	co-ordinate Y, axis Y parallel to radial direction of the ring
		the origin of the co-ordinate system X-Y is at the intersection of e-beam orbit and the exit of upstream dipole magnet (B1)
α	(degree °)	angle between X-ray and e-beam orbit
β	(degree °)	X-ray incidence angle on the absorbers
σ	(mm)	Gaussian vertical height of X-ray
Pl	(W/mm)	linear power density on the absorber in the horizontal plan
Pa	(W/mm2)	surface power density on the absorber
Ptot	(W)	total power on the absorber
CV n° / drawing n°		name of vacuum chamber / number of corresponding drawing

-COMMON PART CELLS-
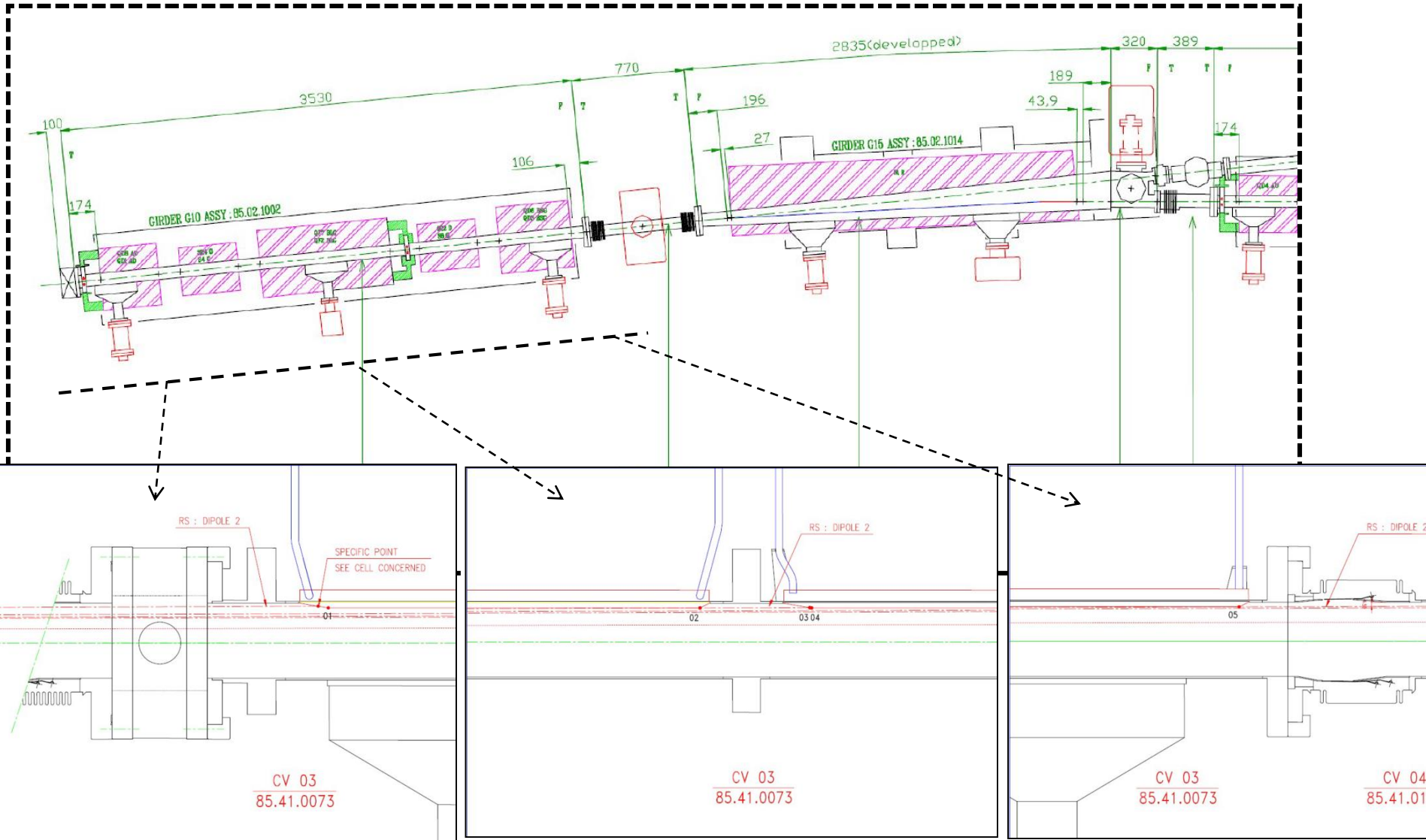from CV03 to CV15

(except CELL 03-04-07-15)
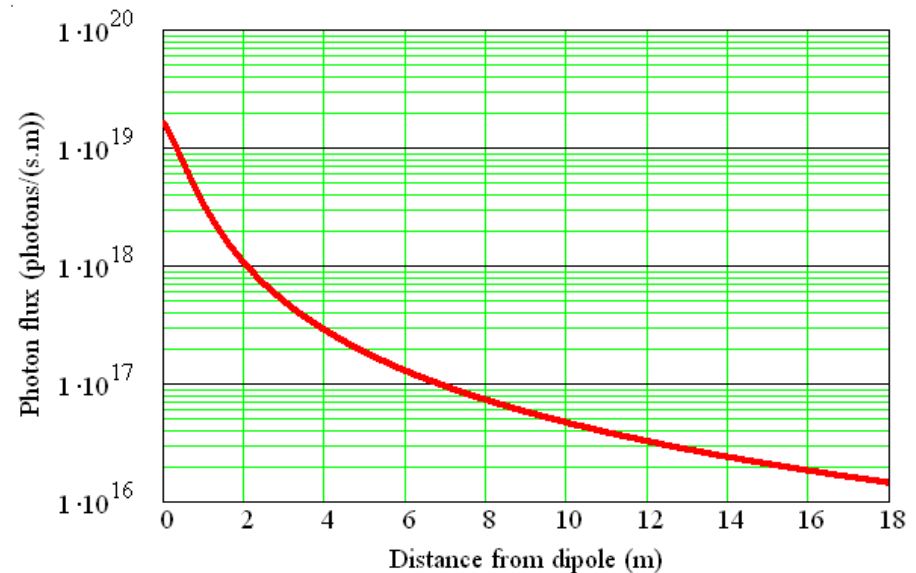
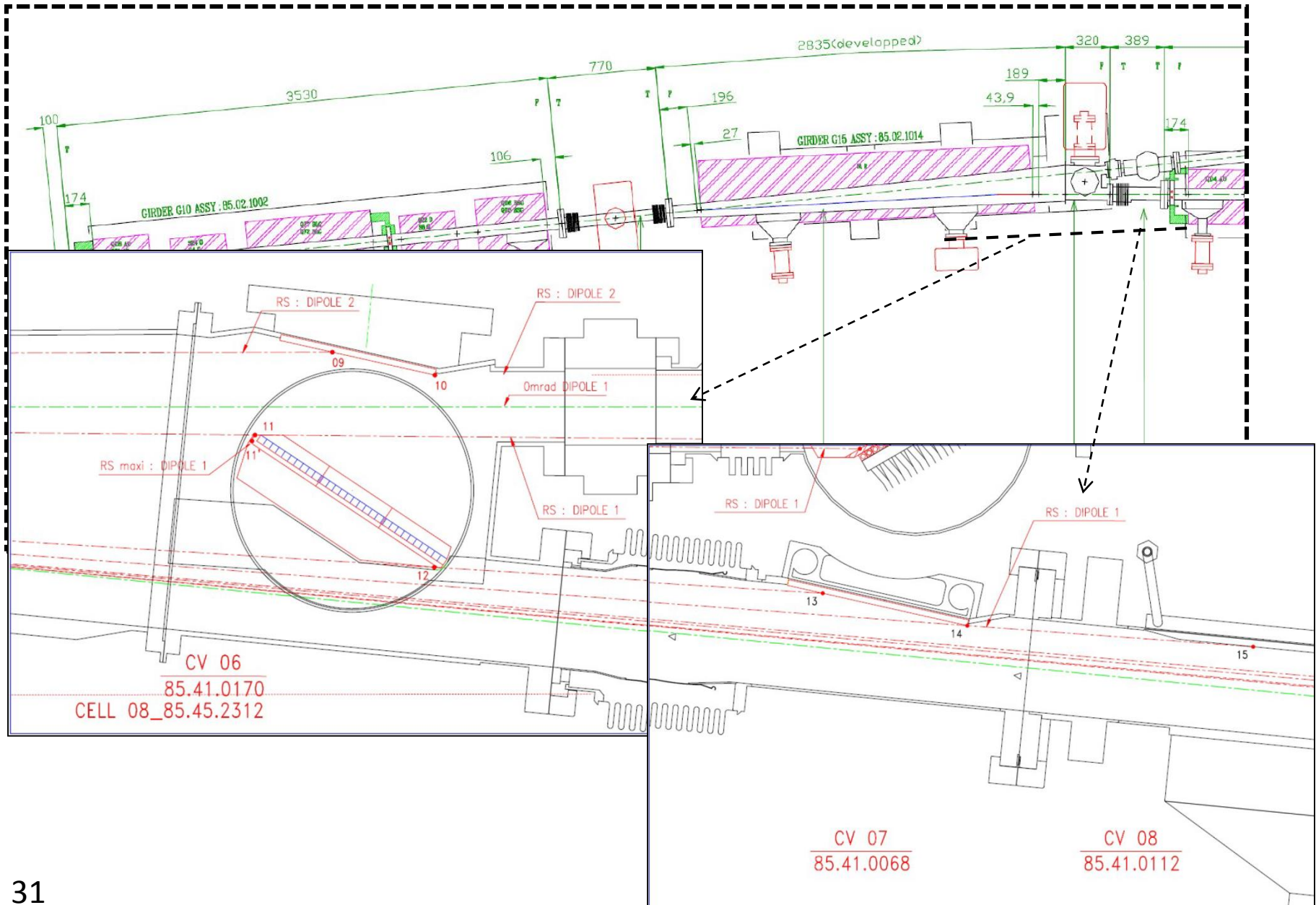Source: O.B. Malyshev, pers. comm.

28

ESRF, 3rd generation synchrotron radiation light source:

29

ESRF, 3rd generation synchrotron radiation light source:

ESRF, 3rd generation synchrotron radiation light source:

31

ESRF, 3rd generation synchrotron radiation light source:

Optimization of the pumping geometry for the new crotch absorber of the ESRF; **doubly-inclined teeth, to reduce the power density**

Change of position of IP/NEG pump and orientation of abs jaws

present version (300 mA max)

from previous dipole

to front-end / beamline

A

B

new version (up to 500 mA)
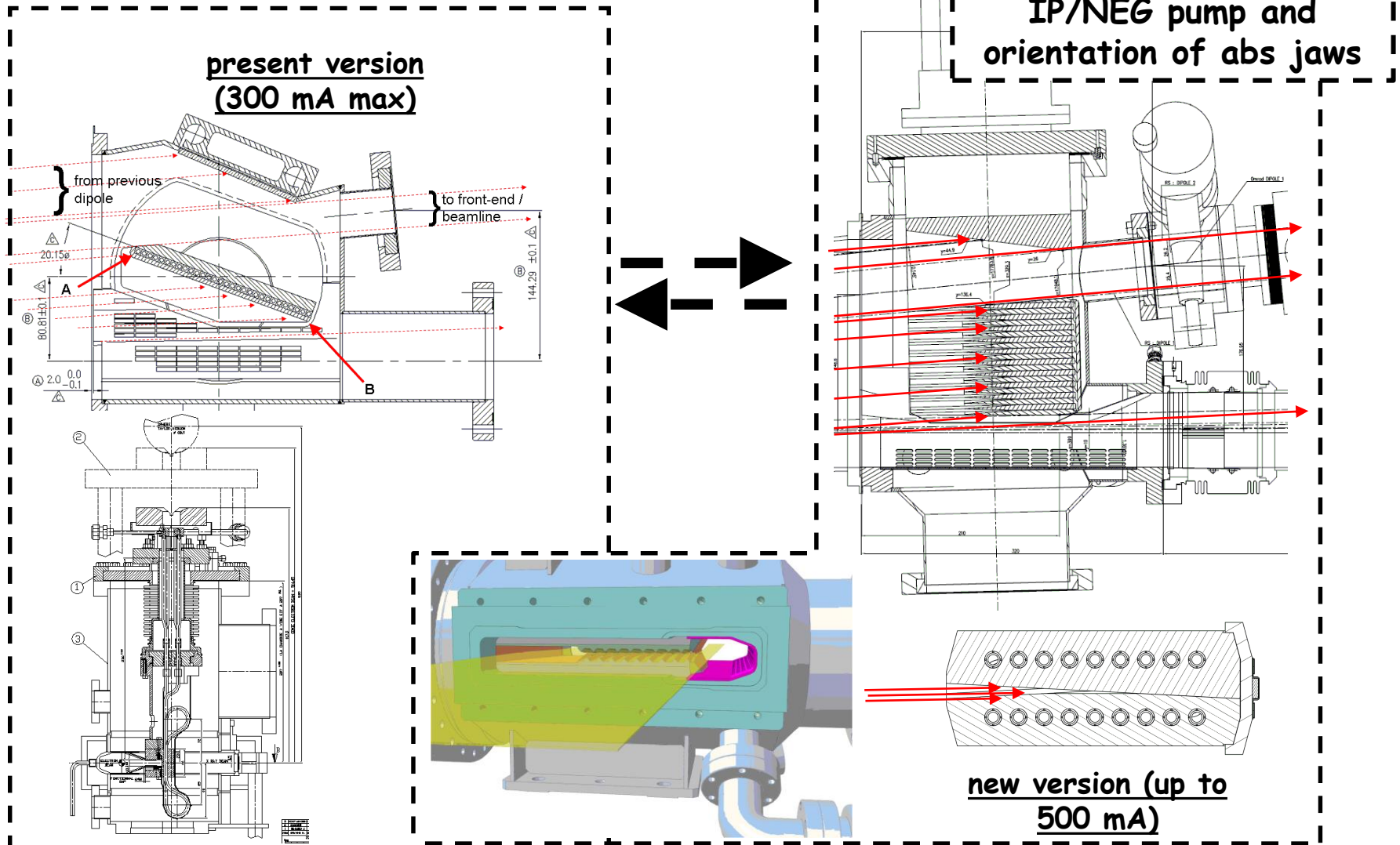
ESRF, 3rd generation synchrotron radiation light source:

Synchrotron Radiation Power Distribution on the Absorbers in the ESRF Storage Ring : *Standard part of a Cell*

*common parts for all cells except cell 03-04-07-15*

E=6 GeV, I=200 mA

64 bending magnets with soft end : B=0.857 T, B(softend)=0.40 T

Vertical emittance =4E-11 m.rad, Vertical dimension at source point 37 μm, Angular deviation =1.07 μrad

Pt n°	Src	Src n°	X mm	Y mm	α °	β °	σ mm	Pl W/mm	Pa W/mm2	Ptot W	CV n° / drawing n°
1		2	10 614	37.00	0.199	0.199	0.912	0.05	0.02		
2		2	12 728	37.00	0.166	0.166	1.090	0.04	0.01		
3	2H	2	12 846	37.34	0.166	9.628	1.101	2.03	0.73	130	CV 03 / 85.41.0073
4		2	12 848	37.00	0.165	9.627	1.101	2.02	0.73		
5		2	13 965	37.00	0.151	0.151	1.195	0.03	0.01		
6		2	14 200	37.62	0.151	9.614	1.215	1.83	0.60		
7	2H	2	14 204	37.00	0.149	9.611	1.216	1.83	0.60	18	CV 04 / 85.41.0107
8		2	14 620	37.00	0.145	0.145	1.251	0.03	0.01		
9	2H	2	17 750	44.90	0.145	12.770	1.517	1.94	0.51	167	CV 06 / fixed absorber
10	2H	2	17 835	26.00	0.083	12.708	1.522	1.93	0.50		85.41.0170
11	1H	1	249	127.02	5.064	56.936	0.214	52.90	98.51	8 160	CV 06 / crotch absorber
11'	1H	1	247	121.48	4.939	90.000	0.210	64.51	122.71		85.41.0170
12	1H	1	406	35.20	2.074	30.074	0.126	55.65	176.88		
6_a	2H	2	18 273	26.64	0.083	29.917	1.560	4.26	1.09		
6_b	2H	2	18 227	0.00	0.000	30.000	1.553	4.29	1.10	1 759	Beam Port
6_b'	1H	1	781	204.89	5.625	150.000	0.279	24.11	34.52		
6_c	1H	1	732	169.79	5.064	149.789	0.255	26.57	41.57		
13	1H	1	717	46.46	2.074	9.074	0.151	14.34	37.88	1 833	CV 07 / 85.41.0068
14		1	843	31.00	1.403	8.403	0.139	14.54	41.79		

ESRF, 3rd generation synchrotron radiation light source:
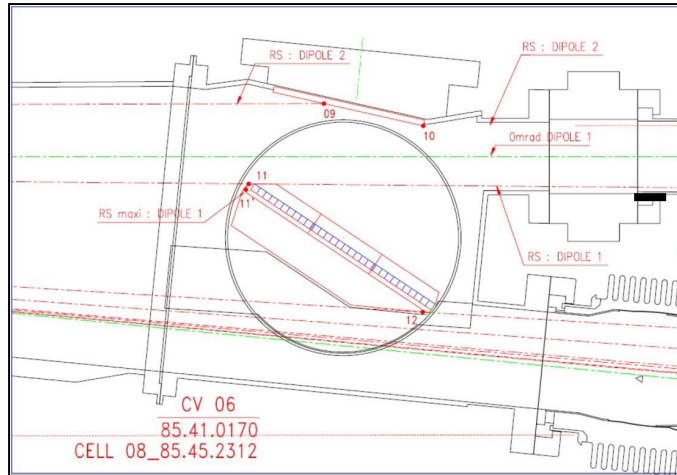
The CAD drawing/model is imported into a MC code (Molflow in this case) which is then run in order to calculate conductances, pressure, pumping speeds, etc...
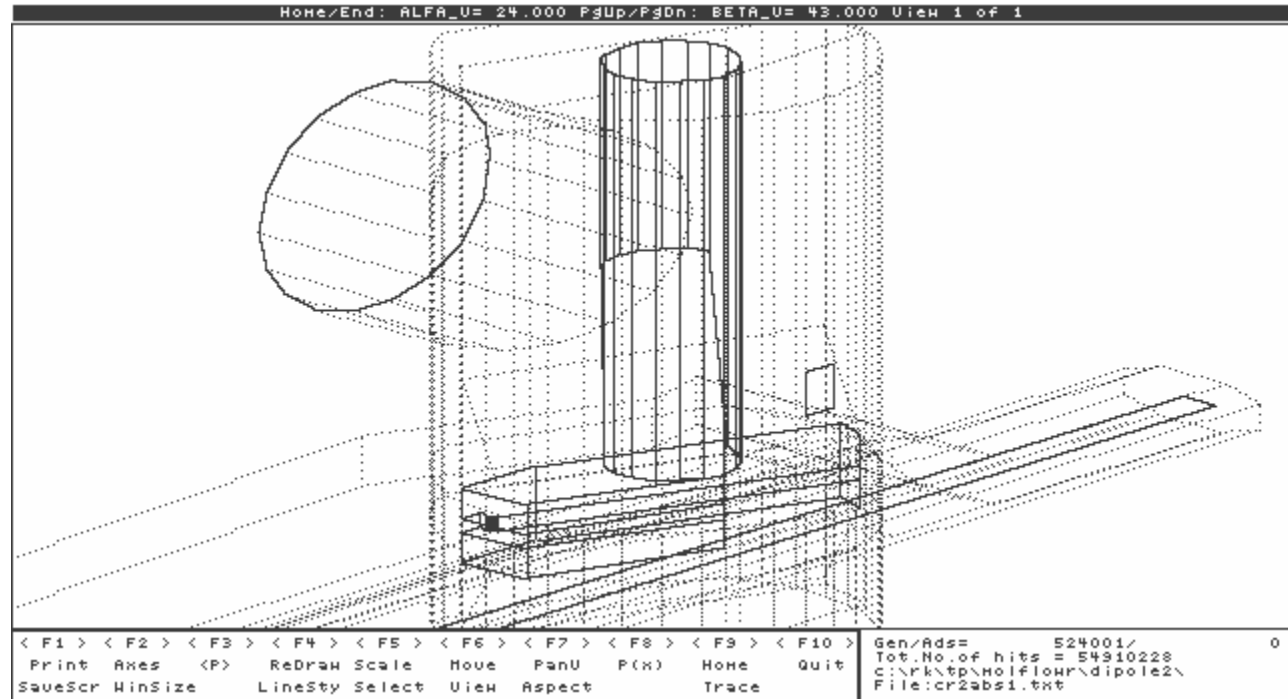
Vacuum Conclusions of SR Analysis:

LHC:

Cryogenic machine, therefore…

-> Limit thermal load to cryo system

-> Large radius of curvature in dipoles

-> Low critical energy, linear power and density (W/m and W/mm^2) , <u>no special absorbers needed</u>

-> Intercept SR on beam-screen at higher T

-> Mask cold bore from SR

-> Use "built-in" cryopump to take care of outgassing (in cold arcs), and NEG-coated chambers in Long-Straight Sections (room Temp.)

ESRF:

Room temperature machine, with high-brightness beam, optimized to generate SR, therefore…

-> Absorb 100% of SR on carefully designed absorbers

-> Make accurate analysis of SR power, linear and density (W/m and W/mm^2), <u>custom absorbers needed!</u>

-> Beware of power densities exceeding SR absorbers' material specs!

-> Install as many pumps as possible along the machine

-> Use NEG-coated chambers in places where low-conductance chambers cannot be avoided (e.g. undulators, wigglers)
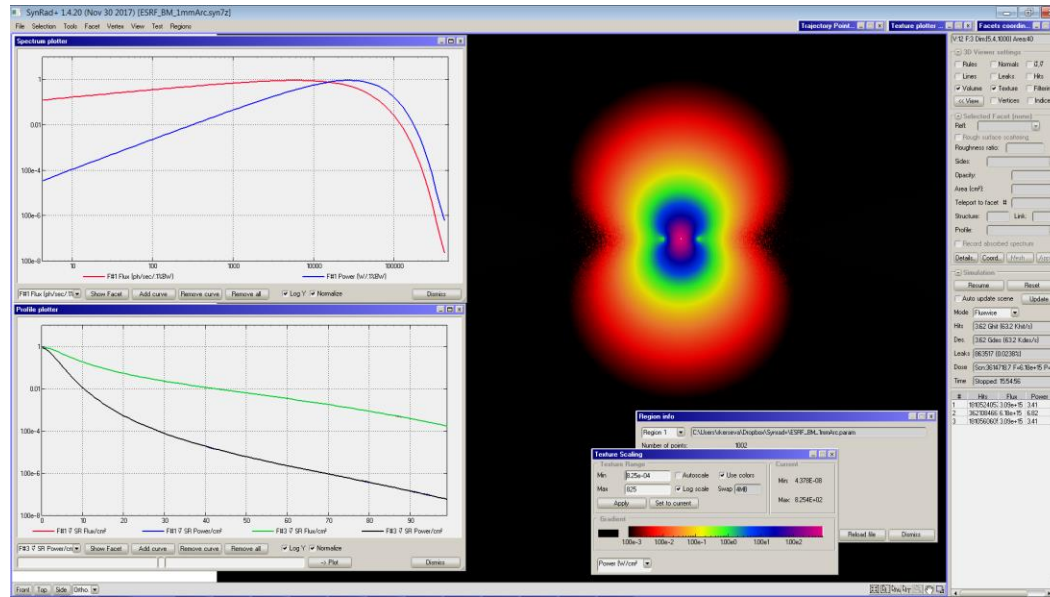
Total power (up), Parallel Polarization (bottom left), and Vertical Polarization (bottom right)